RADIATION DETECTORS:
IMAGING WHAT YOU CANNOT SEE

Cinzia Da Vià
The University of Manchester, UK & Stony Brook University USA

Some Information about myself

- Professor at The University of Manchester (UK)
- Visiting Professor at the University of Stony Brook, New York, USA
- Member of the ATLAS Collaboration at CERN – LHC
- Chief editor Frontiers in Physics, Radiation detectors and Imaging
- IEEE WIE International Committee Member @WIE@25 Chair
- Member of the IEEE TAB Program on Climate Change
- IEEE NPSS WIE Liaison
- Distinguished Lecturer and Organizer of the IEEE NPSS Instrumentation School

With Joyce Mwangama
WIE South Arfrica and
R8 WIE Rep 2018
Organizing a WIE event with local students
Cape Town July 2018

Scientific Interests:

- Radiation Detector development : silicon pixels, fast timing
- Radiation effects in silicon, Lazarus effect
- 3D sensors for high energy physics and other applications
- 3D printed detectors, Vertical integrated microsystems
- Quantum Imaging

Imaging radiation ..

Web cams

Smart phones

photo cameras

machine vision, automotive, security etc…

Medical imaging

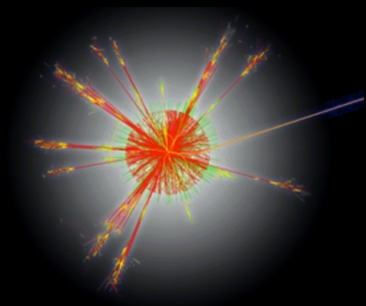

HEP

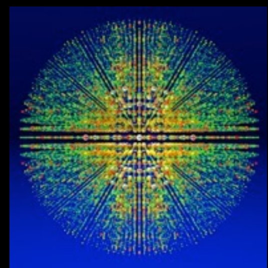

x-ray crystallography

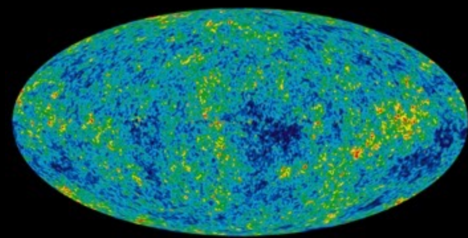

cosmology   ……

mass spectroscopy, neutrons, electrons, TOF, SEM/TEM etc…

Cinzia Da Via, Stony Brook USA and The University of Manchester, UK– 2022

What is Radiation and its interaction with matter

Radiation can be defined as the propagation of energy through space or matter in the form of electromagnetic waves or energetic particles.

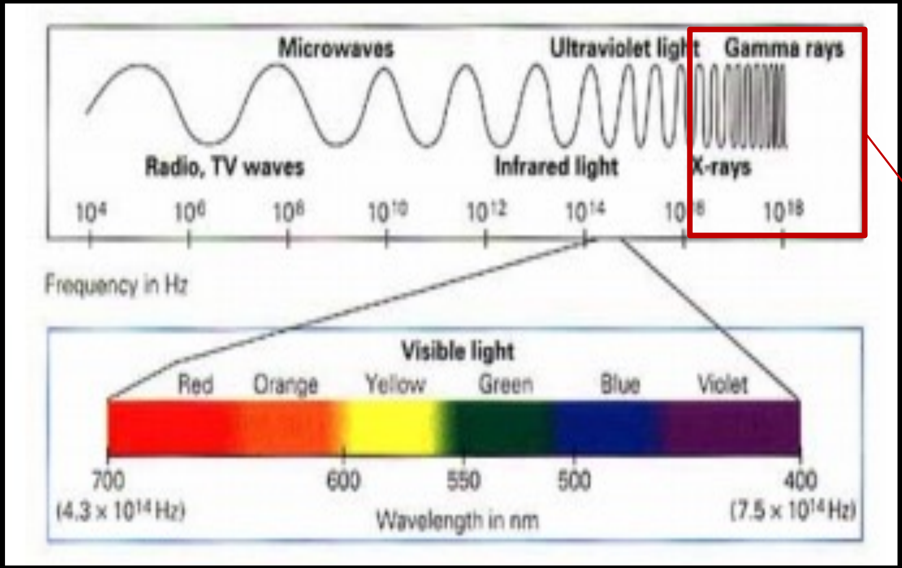

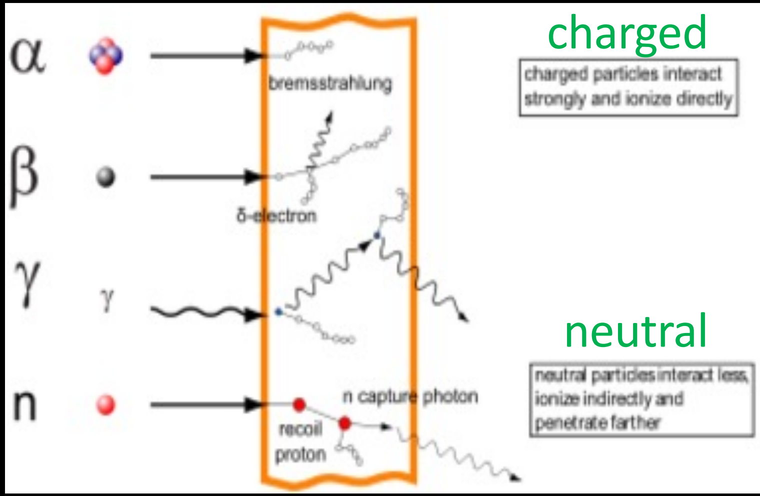

When radiation interacts with matter:

Non-ionizing does not have enough energy to ionize atoms but generate heat in the material it interacts with. At high energy it becomes ionizing

Ionizing
has the ability to knock an electron from an atom, i.e. to ionize..

Interaction of radiation with matter

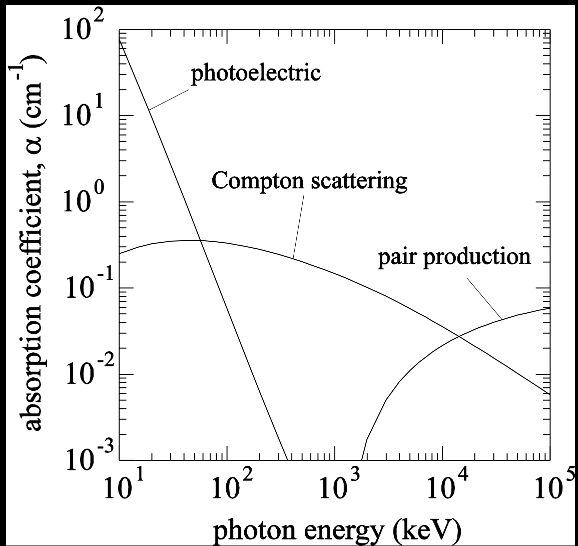

Photons:

There are 3 main modes of interaction:
-Photoelectric absorption
-Electron scattering
-Pair production

Lambert-Beer’ s law

$$\phi(x) = \phi_0 \cdot e^{-\alpha x}$$

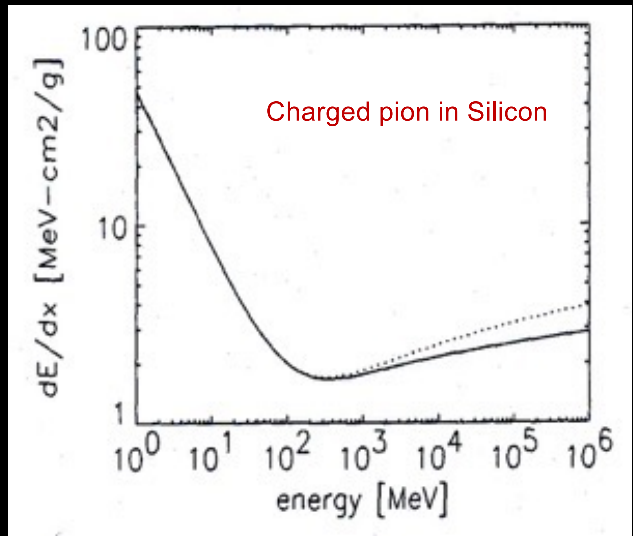

Ionizing particles:

Bethe-Bloch equation:
average/mean amount of energy lost due to ionization per unit of distance in the media)

$$-\frac{dE}{dx} = \frac{4\pi}{m_e c^2} \cdot \frac{nz^2}{\beta^2} \cdot \left(\frac{e^2}{4\pi\varepsilon_0}\right)^2 \cdot \left[\ln\left(\frac{2m_e c^2 \beta^2}{I \cdot (1-\beta^2)}\right) - \beta^2\right]$$

$$n = \frac{N_A \cdot Z \cdot \rho}{A \cdot M_u}$$

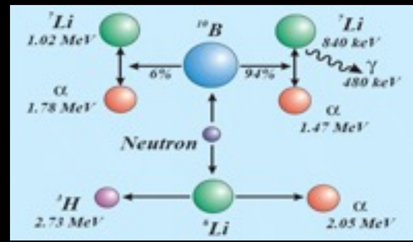

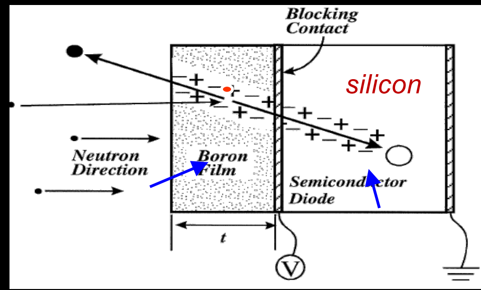

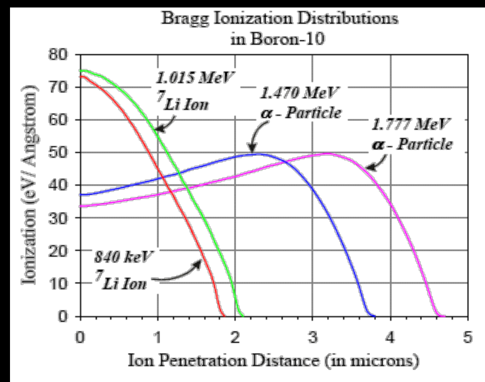

Neutrons: Alpha Bragg peak

Cinzia Da Via, Stony Brook USA and The University of Manchester, UK– 2022

Particle “signatures” with the Timepix readout electronics

α	5 KeV X-rays	2MeV electrons
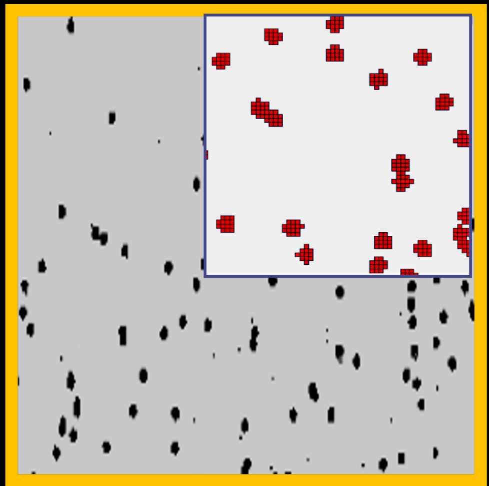	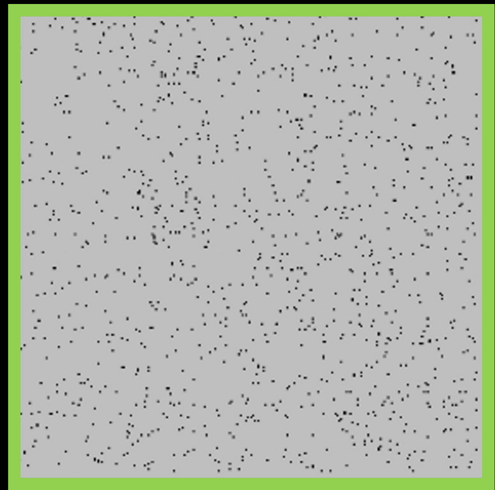	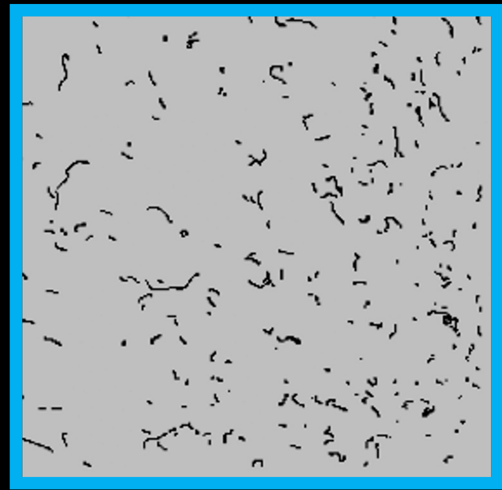

- ^{241}Am alpha source gives clusters of ~5x5 pixels measured with the MEDIPIX-USB device and a 300 µm thick silicon sensor. The clusters are shown in detail in the inlet. The cluster sizes depend on particle energy and threshold setting.
- Signature of X-rays from a ^{55}Fe X-ray source. Photons yield single pixel hits or hits on 2 adjacent pixels due to charge sharing.
- A ^{90}Sr beta source produces curved tracks in the silicon detector.
- A pixel counter is used just to say “YES” if individual quantum of radiation generates in the pixel a charge above the pre-selected threshold

How things started...

Cinzia Da Via, Stony Brook USA and The University of Manchester, UK– 2022

1896 : Therapeutic use of X-rays
1903 : Authored first textbook of radiotherapy

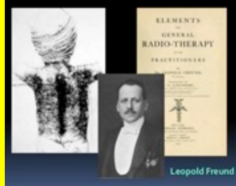

A five yr old girl with pigmented hairy naevus all over her back treated and cured, then lived upto 75 yrs.

1897 : Discovery of Electrons by J . J . Thompson

Received Nobel Prize in Physics 1906

1899: Discovery of α & β particles (E. Rutherford)
1900: Proposal of Radioactive Decay & Half life

Received Noble prize in Chemistry 1908 for "Disintegration theory" of elements

Wilhelm Conrad Röntgen: Discovery of X-ray (November 8 ,1895)

1996 Becquerel discovers spontaneous radioactivity

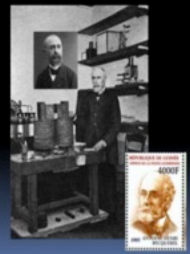

The Nobel Prize in Physics 1903.......awarded to Antoine Henri Becquerel "in recognition of the extraordinary services he has rendered by his discovery of spontaneous radioactivity"

1898: Discovery of Radium And Polonium

Marie and Pierre Curie shared 1903 Nobel prize in physics with Becquerel

1800es | 1895 | 1896 | 1897 | 1898 | 1899

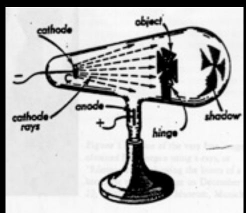

Hittorf-Crookes tube

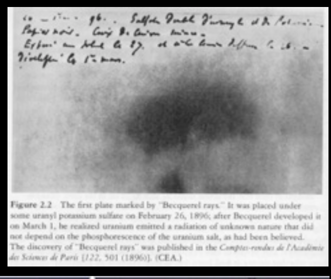

Photographic plate
Used to study "x-rays".. But they deflected with B-field

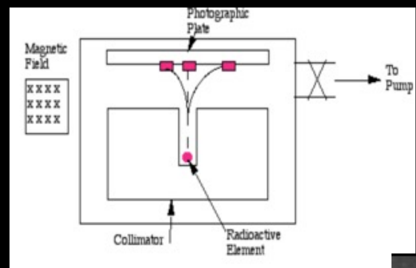

1908-1913
Geiger-Masden Apparatus
Or Rutherford Gold foil Experiment proved the atomic structure

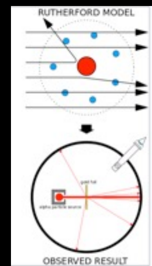

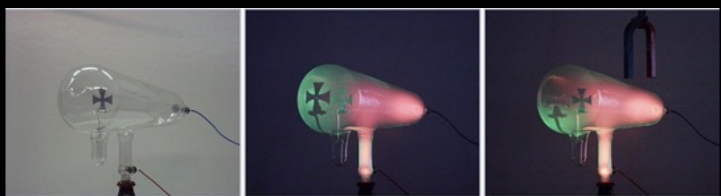

Power off. | Without magnet, rays travel straight. | With magnet, rays are bent down.

Cathode rays (e^-)
Deflected by B field

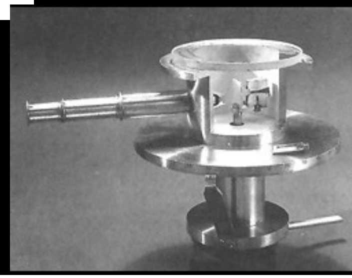

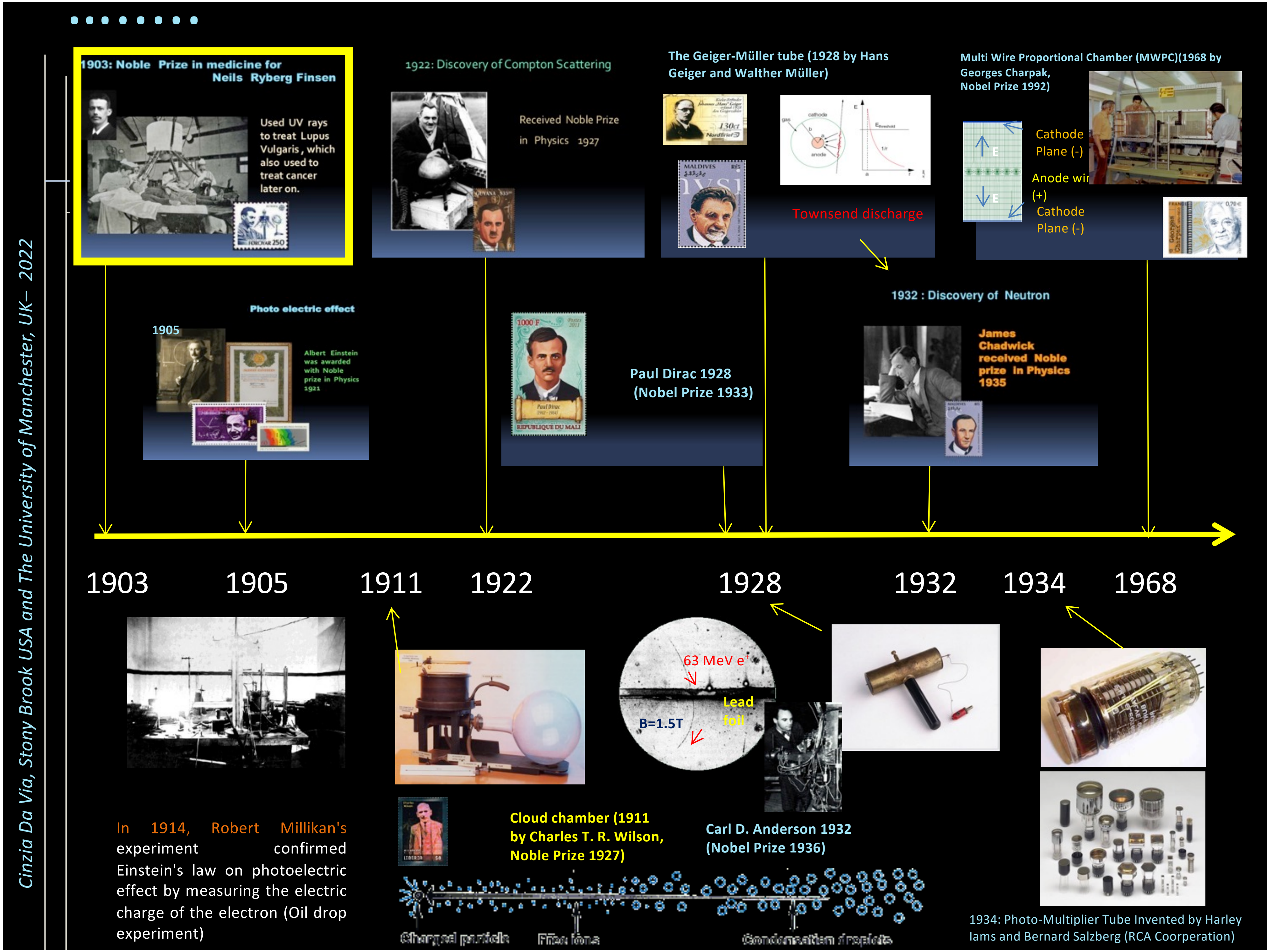
Cinzia Da Via, Stony Brook USA and The University of Manchester, UK– 2022
1903: Noble Prize in medicine for Neils Ryberg Finsen
Used UV rays to treat Lupus Vulgaris, which also used to treat cancer later on.
1922: Discovery of Compton Scattering
Received Noble Prize in Physics 1927
The Geiger-Müller tube (1928 by Hans Geiger and Walther Müller)
Townsend discharge
Multi Wire Proportional Chamber (MWPC)(1968 by Georges Charpak, Nobel Prize 1992)
Cathode Plane (-)
Anode wi
(+)
Cathode Plane (-)
Photo electric effect
1905
Albert Einstein was awarded with Noble prize in Physics 1921
Paul Dirac 1928 (Nobel Prize 1933)
1932 : Discovery of Neutron
James Chadwick received Noble prize in Physics 1935
1903
1905
1911
1922
1928
1932
1934
1968
In 1914, Robert Millikan's experiment confirmed Einstein's law on photoelectric effect by measuring the electric charge of the electron (Oil drop experiment)
Cloud chamber (1911 by Charles T. R. Wilson, Noble Prize 1927)
63 MeV e+
Lead foil
B=1.5T
Carl D. Anderson 1932 (Nobel Prize 1936)
Charged particle
Free ions
Condensation droplets
1934: Photo-Multiplier Tube Invented by Harley Iams and Bernard Salzberg (RCA Coorperation)

The semiconductor revolution 1947

First transistor invented 1947 by William B. Shockley, John Bardeen and Walter Brattain (Nobel Prize 1956)

First semiconductor particle sensor: Pieter Jacobus Van Heerden, *The Crystalcounter: A New Instrument in Nuclear Physics.* University Math Naturwiss, Fak (1945).

CCD Nobel prize Boyle Smith 2009

Semiconductor a material that has a conductivity between a conductor and an insulator; electricity can pass through it, but not very easily

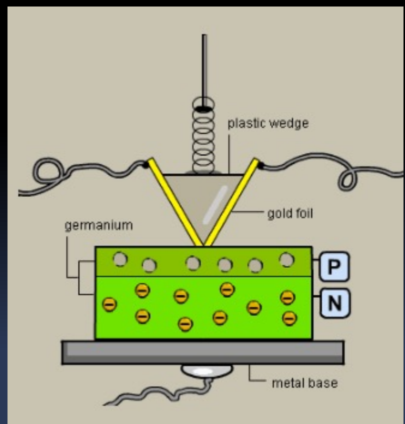

The point contact germanium transistor

p-n junction

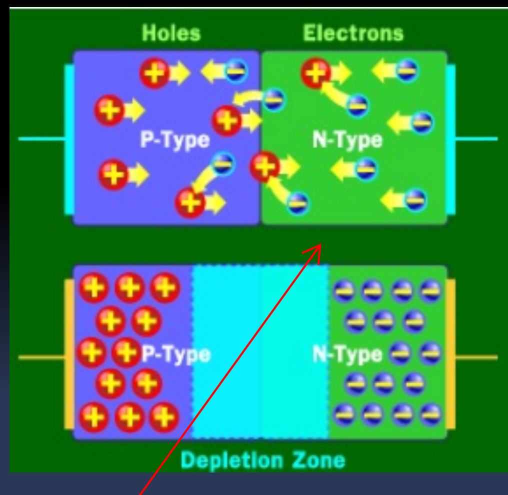

Depleted region particle yes/no

particle

Cinzia Da Via, Stony Brook USA and The University of Manchester, UK– 2022

Why Silicon is still the most used material

- Semiconductor with Low ionization energy → big signal
  The band gap is 1.12 eV, but it takes 3.6 eV to ionize an atom. The remaining energy goes to phonon excitations (heat)

- **High purity → long carrier lifetime**

- High mobility →fast charge collection

- Low Z→ Z=14 low multiple scattering but low x-ray detection efficiency

- Oxide (SiO_2) has excellent electrical properties

- Good mechanical properties→ Easily patterned to small dimensions

- Can be operated in air and at room temperature (before irradiation –afterwards requires cooling)

- Industrial experience and commercial applications

- **Silicon is abundant! Over 90% of the Earth's crust is composed of <u>silicate minerals</u>**

making silicon the second most abundant element in the Earth's crust (about 28% by mass) after oxygen

Parameter	cBN	hBN	Diamond	AlN	GaN	3C-SiC	GaAs	Si
Energy Bandgap (eV)	6.4	5.2	5.45	6.2	3.39	3.00	1.43	1.12
Electron Mobility (cm^2/Vs)	280	-	2200	300	440	400	8500	1500
Hole Mobility (cm^2/Vs)	-	-	1600	30	~20	50	400	600
Thermal Conductivity (W/cm K)	13	a = 6.0 c = 0.3	20	2.9	1.3	5	0.46	1.5
Breakdown ($\times 10^5$ Vcm^{-1})	~80	~80	100	~80	~80	40	60	3
Lattice Constant (Å)	3.615	a = 2.504 c = 6.661	3.567	4.982	a = 3.189 c = 5.185	4.358	5.65	5.43
Thermal Expansion Coefficient ($\times 10^{-6}$ ℃$^{-1}$)	3.5	a = -2.7 c = 38	1.1	4.0	4.5	4.7	5.9	2.6
Density (gm/cm^3)	3.487	2.28	3.515	3.26	6.15	3.216	5.316	2.328
Melting Point (℃)	2973	3000	3800	2200	>2500	2540	1238	1420
Dielectric Constant	7.1	5.1	5.5	-	9.5	9.7	12.5	11.8
Resistivity (Ω cm)	10^{16}	10^{10}	10^{13}	10^{14}	10^{12}	150	10^8	10^3
Absorption Edge (μm)	0.205	0.212	0.20	-	0.35	0.40	-	1.40
Refractive Index	2.17	1.80	2.42	2.00	2.33	2.65	3.4	3.5
Hardness (kg/mm^2), $T = 300$ K Kg/mm^2	5000	100	10,000	2500	1100	3000	600	1000

Cinzia Da Via, Stony Brook USA and The University of Manchester, UK– 2022

SILICON: from sand to wafer

a) The sand is cleaned and further purified by chemical processes. It is then melted. Then a tiny concentration of phosphorus (boron) dopant is added to make n (p) type poly-crystalline ingots

b) Single-crystal silicon is obtained by melting the vertically oriented poly-silicon cylinder onto a single crystal "seed" --- called "Float Zone-→ FZ"

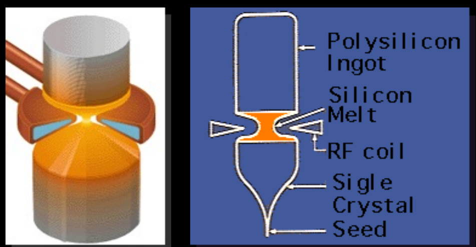

c) Wafers of thickness 200- 500μm are cut with diamond encrusted wire or disc saws.

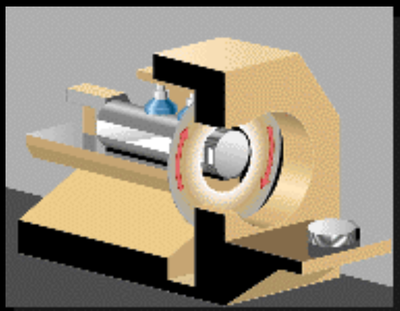

Note: the crystal orientation matters!
<111> and <100> crystals can influence the detector properties eg. capacitance

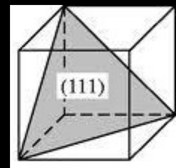

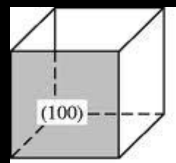

From Wafers to Sensors

Dopants →

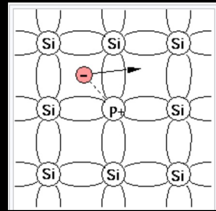

e-

Donors (Phosphorus)

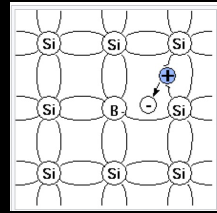

h^+

Acceptors (Boron)

1) 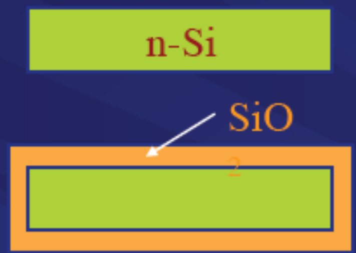

Start with n-doped silicon wafer, $\rho \approx$ 1-10 kΩcm. Silicon can be turned into n-type by neutron doping ($^{30}Si+n \rightarrow {}^{31}Si$, $^{31}Si \rightarrow {}^{31}P+\beta^{-}+\nu$)

2) Oxidation at 800 - 1200°C

3) Photolithography (= mask align + photo-resist layer + developing) followed by etching to make windows in oxide

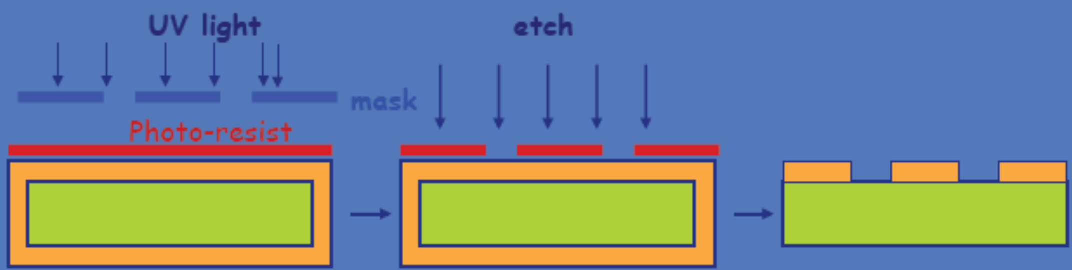

D. Bortoletto Lecture 4 50

Note:

This process is used for single and double side processing

Photo-lithography Followed by Aluminum Deposition in the contact Regions (front and back)

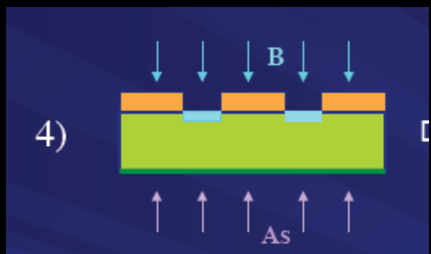

Doping (ion implantation or diffusion)

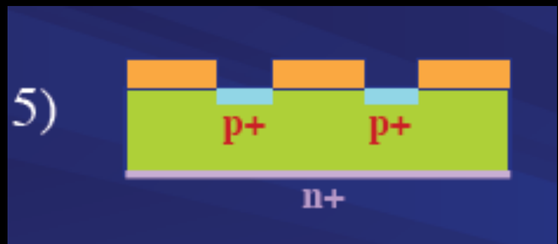

Crystal lattice annealing at 600C

p-n junction detector basic working principle

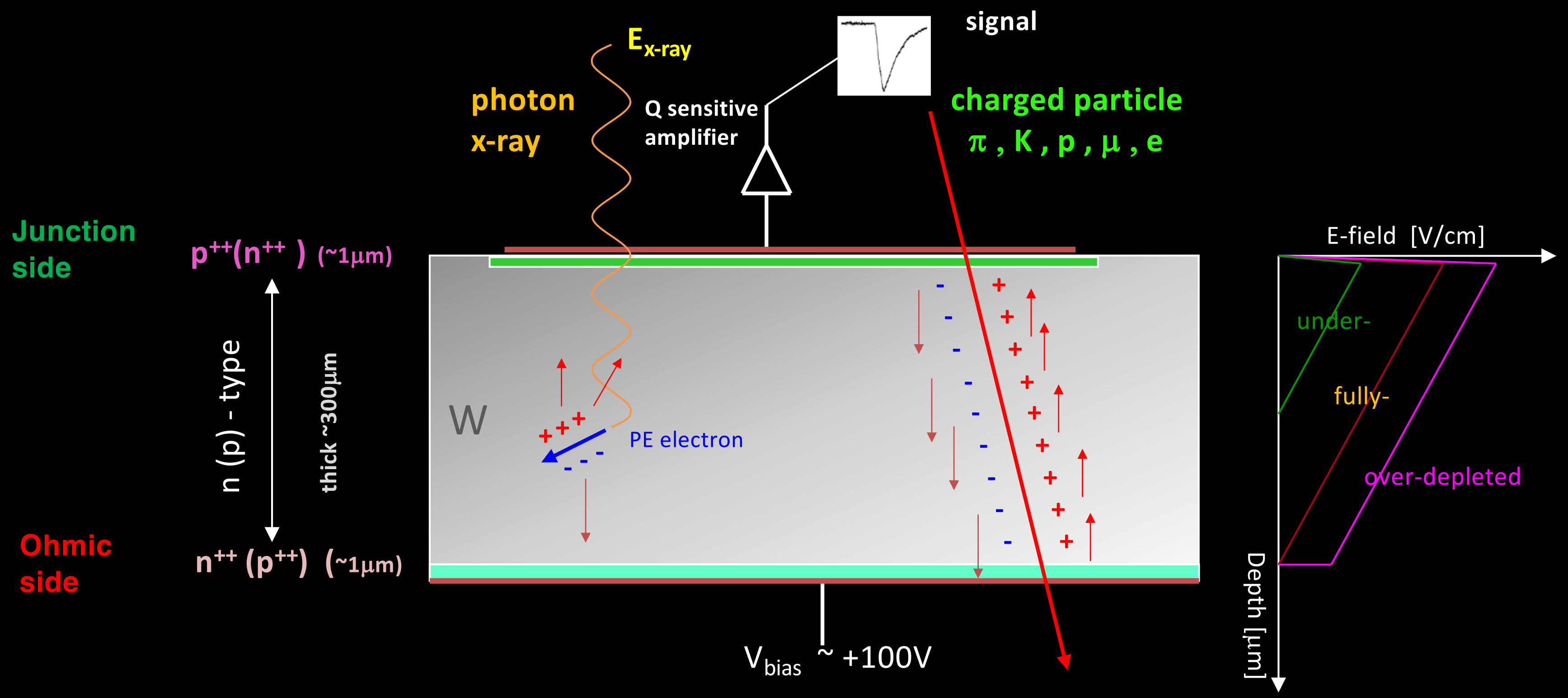

- n+ and p+ electrodes are implanted on the wafer's surfaces to form a p-i-n junction
- V_{bias} is the applied reverse bias voltage, W is the depletion region
- e-h pairs are created by the energy released by the impinging particle
- e-h drift towards the positive and negative electrode "inducing " a current pulse
- Charge collection time depends on the carrier mobility, bias voltage and carrier polarity

$$V_{bias} = \frac{(W)^2 \times e \times |N_{eff}|}{2\varepsilon_0 \varepsilon_{Si}}$$

Cinzia Da Via, Stony Brook USA and The University of Manchester, UK– 2022

Segmented Silicon Sensors for better position sensitivity .."imaging"

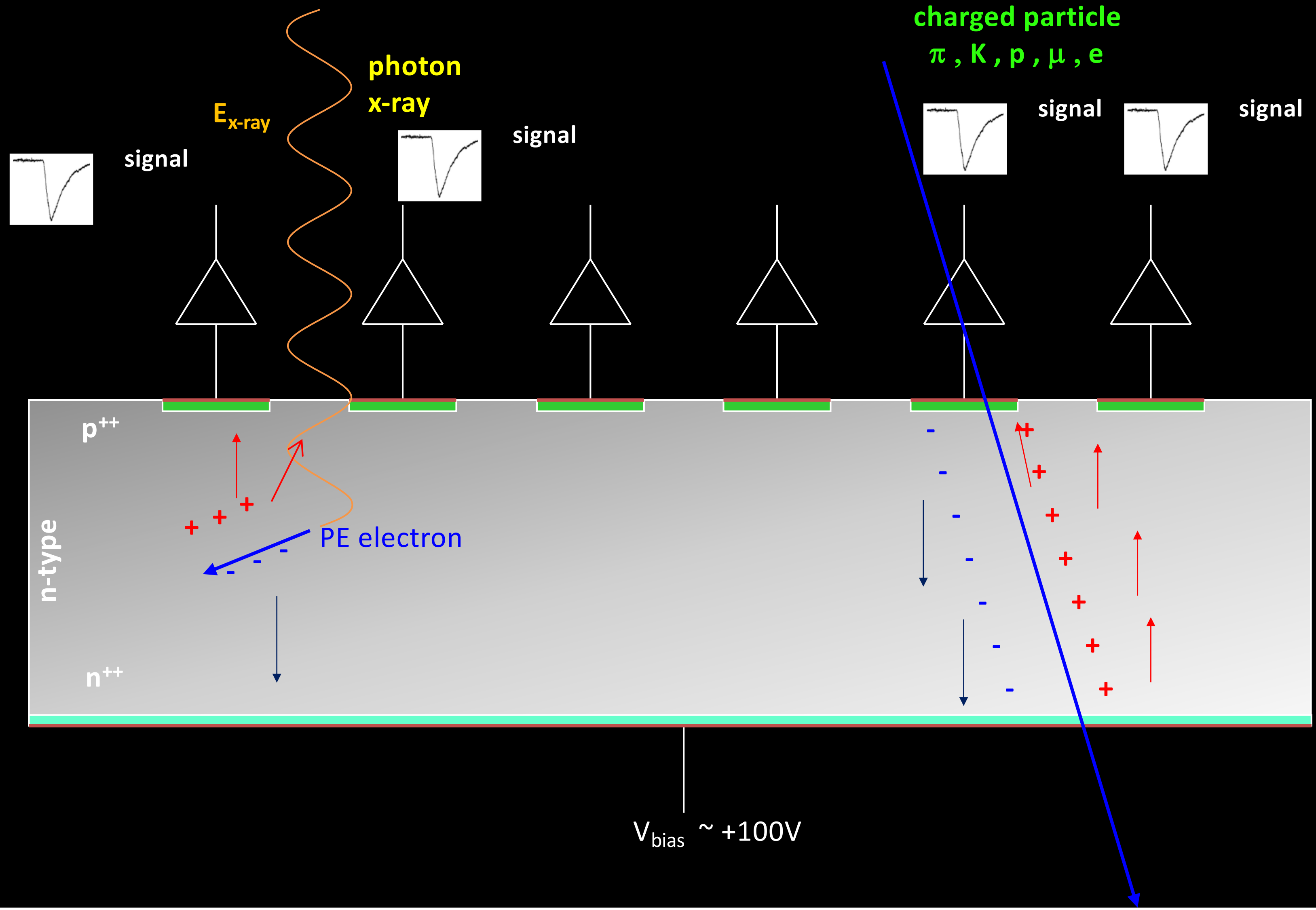

Two dimensional segmentation. Pixel Detectors “Hybrid”

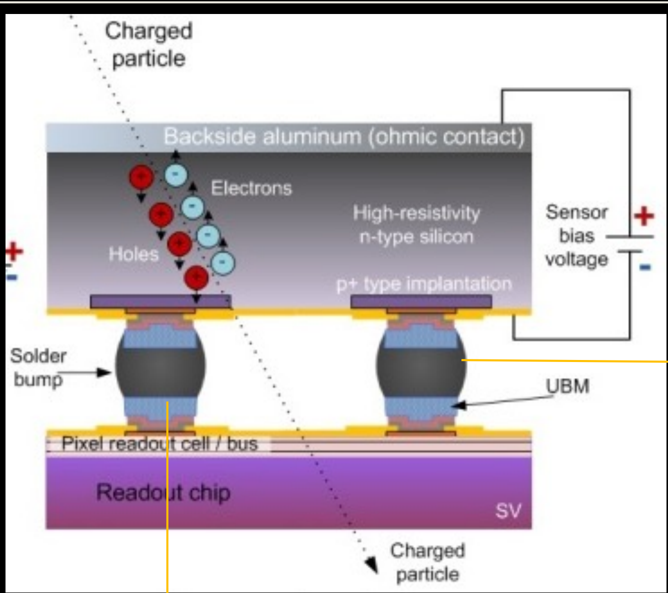

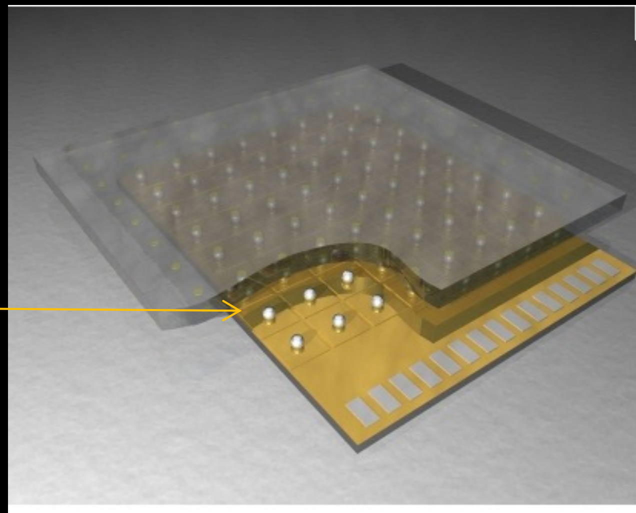

FE-I4
80x336
=26 880 pixels
125 x 50 um^2

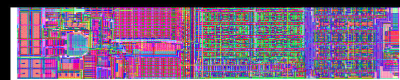

solder

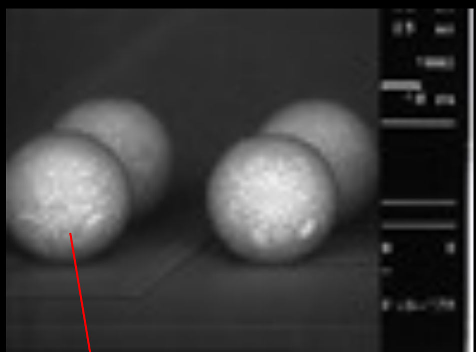

50 microns (25um In, <10um Au)

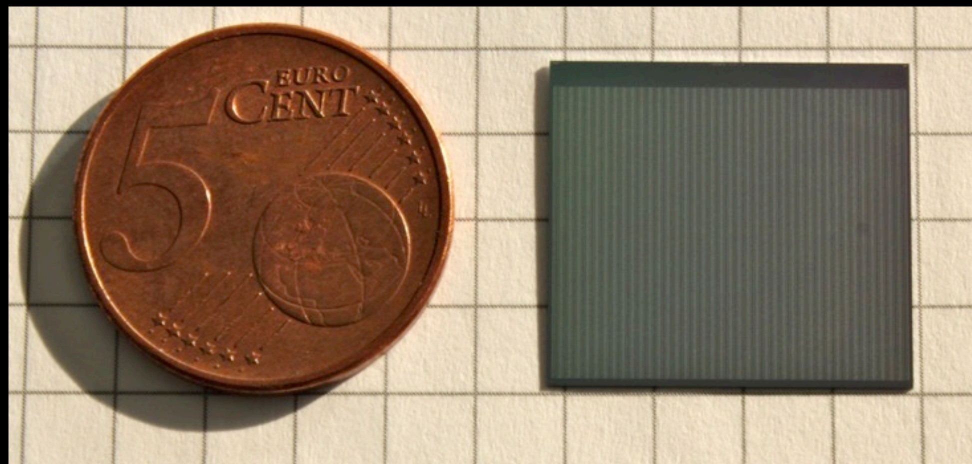

ATLAS FE-I4~4cm^2

Cinzia Da Via, Stony Brook USA and The University of Manchester, UK– 2022

Pixel detectors "Monolithic"

Integrate the readout circuitry together with the detector in 'one piece ' of silicon

The charge generated by a particle is collected on a defined collection electrode either by diffusion or by the application of an E-field

Small pixel size and thin effective detection thickness

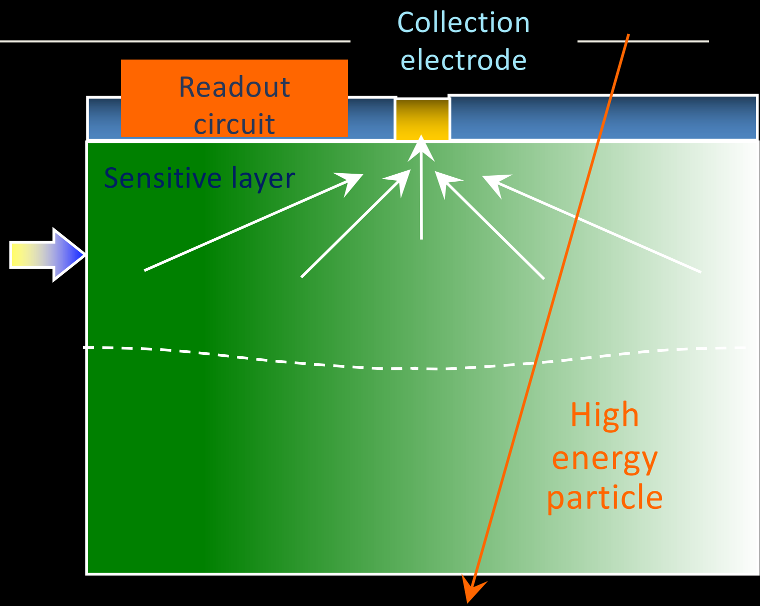

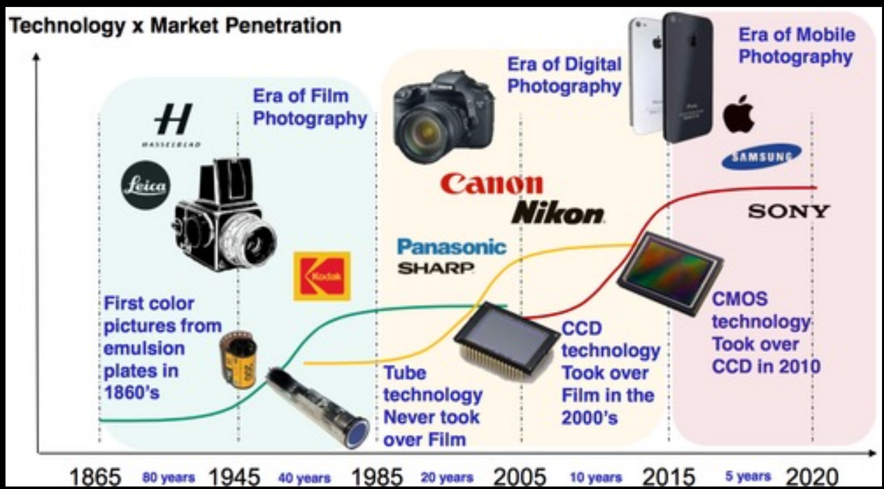

MAPS

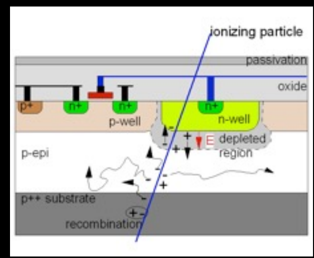

Pixel size :
20 x 20 micron
Thickness
20-50 um

Used in the
EUDET telescope
And at STAR at RICH

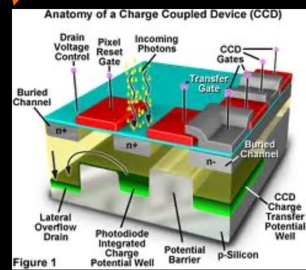

CCD
Charge coupled
Device
Various
dimensions

Many uses in
Different fields

IEEE TNS Vol: 56, Issue: 3, 2009

LGAD Basics. Low Gain Detector

G. Pellegrini, Low Gain Avalanche Detectors

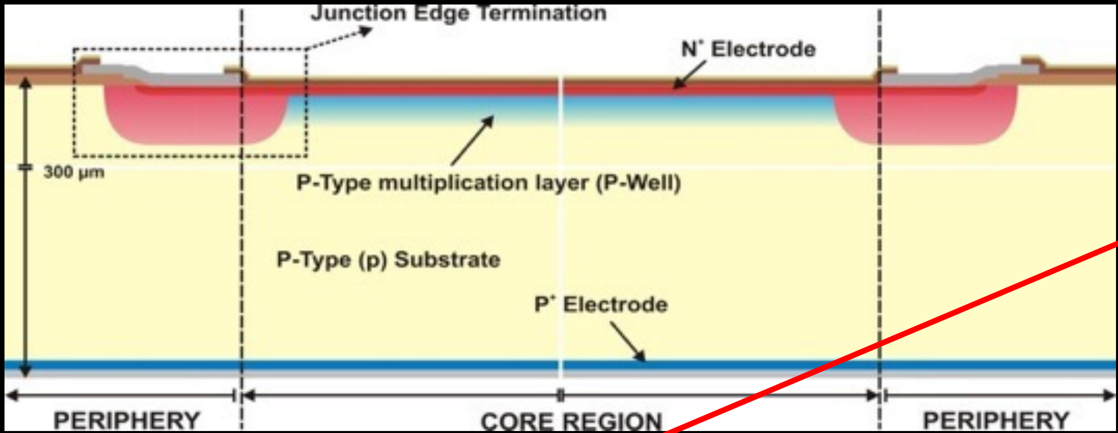

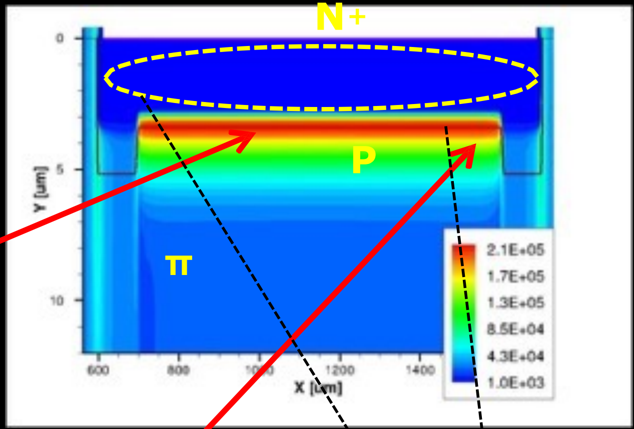

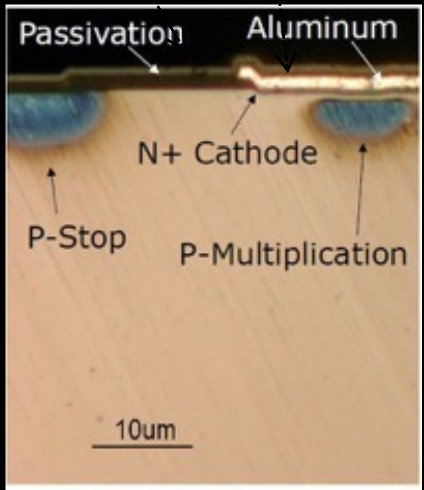

- **Core Region**
  - ✓ **Uniform electric field**, high enough to activate mechanism of **impact ionization** (multiplication)
- **Termination**
  - ✓ **High electric field** confined in the **core region**
- **Periphery**
  - ✓ **Dead region**. **Charges** should not be collected. **Reduction** of the surface **leakage currents**

LGAD Measurements

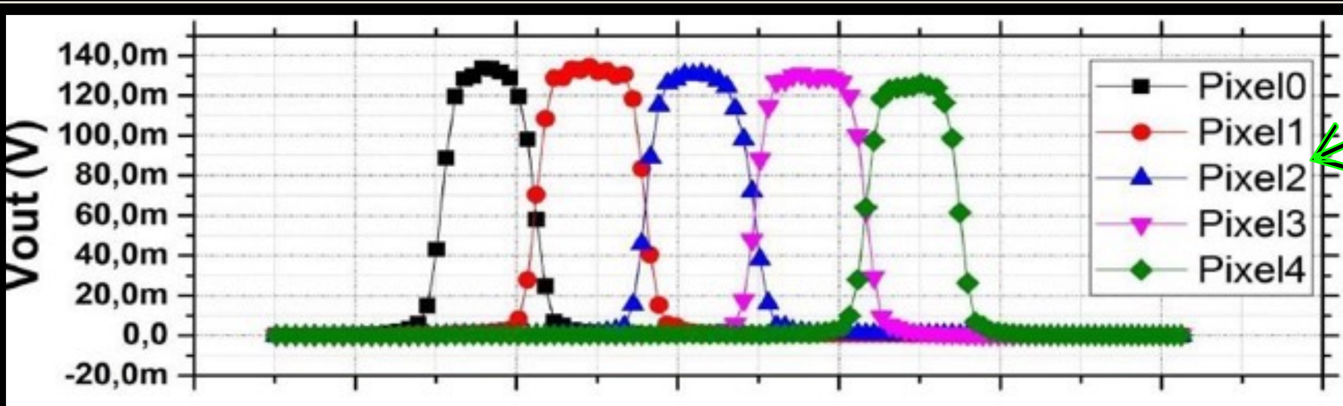

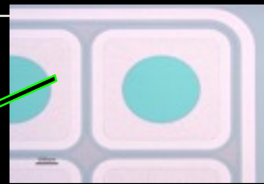

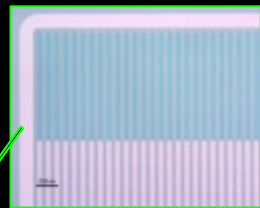

O. Alonso et al., presented at the PIXEL2016 workshop.

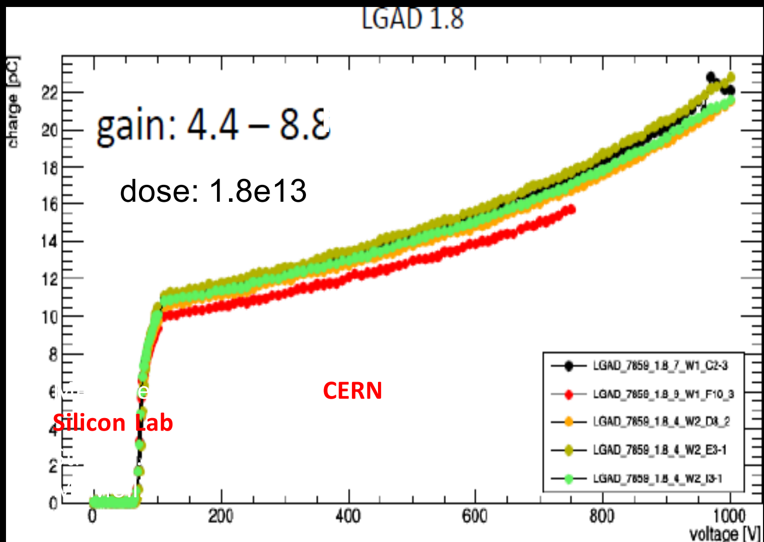

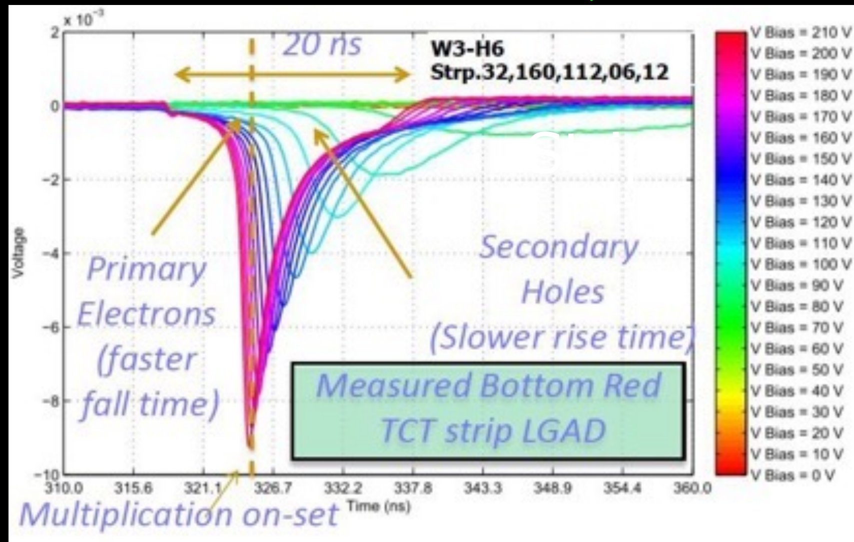

I. Vila, presented at the 28th RD50 workshop

Cinzia Da Via, Stony Brook USA and The University of Manchester, UK– 2022

Electron Multiplied CCD (EMCCD)

https://andor.oxinst.com/products/ixon-emccd-cameras

Electron-multiplying CCDs (EMCCDs) employ on-chip multiplication by impact ionization to multiply the number of photoelectrons, allowing the signal of a single photon to overcome the noise floor, effectively obtaining single-photon detection capability. The multiplication process reduces the effective readout noise below 1 electron but induces an additional noise due to the stochastic variation in the multiplication factor.

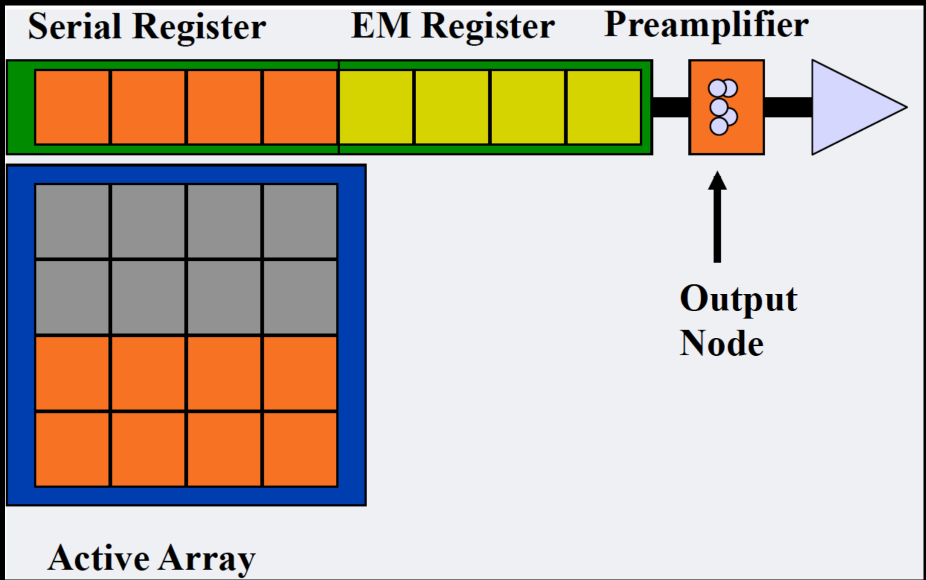

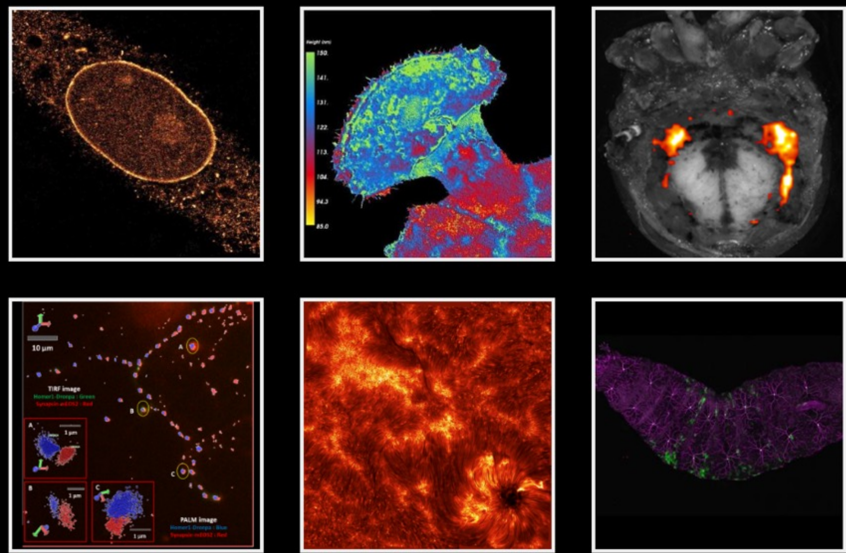

But there are also Gaseous Pixel Detectors!

H. van der Graaf (Nikhef) TIPP2011

Gaseous Pixel detector (GridPix) is a MEMS made Micromegas like structure on a CMOS readout chip

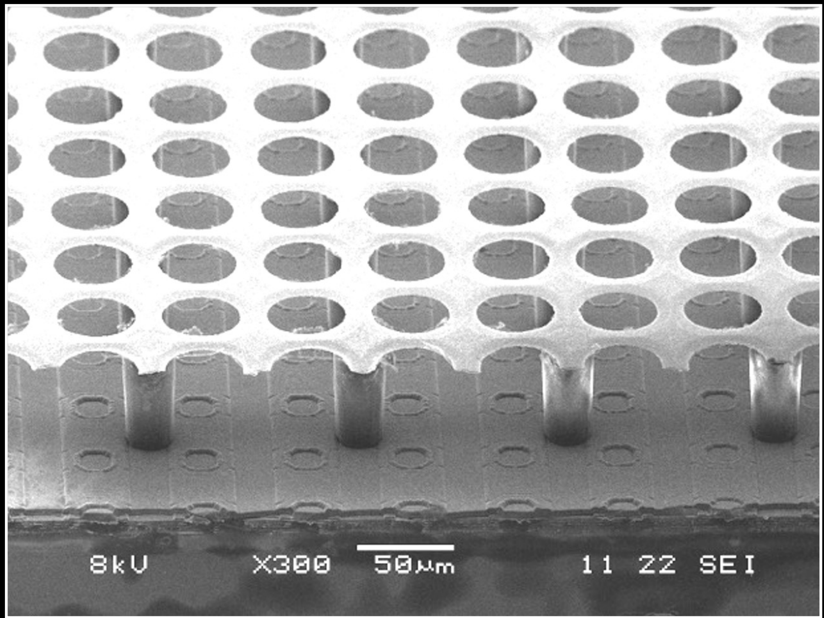

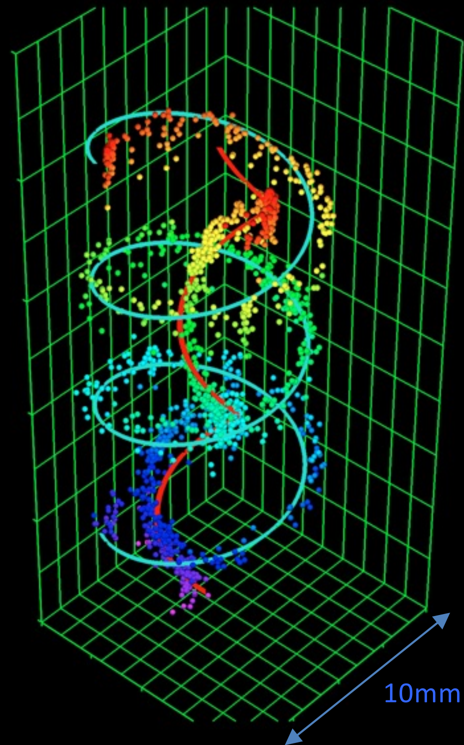

^{90}Sr electrons in 0.2 T B-field

Performance :

- position resolution:15 µm
-single electron efficiency: > 90 %
- track detection efficiency: 99.6 %;

µ-TPC operation with TimePix chip

Applications: Astro-particle Physics…

AMS (Alpha Magnetic Spectrometer)
on ISS particle physics experiment in space
to measure antimatter in cosmic rays

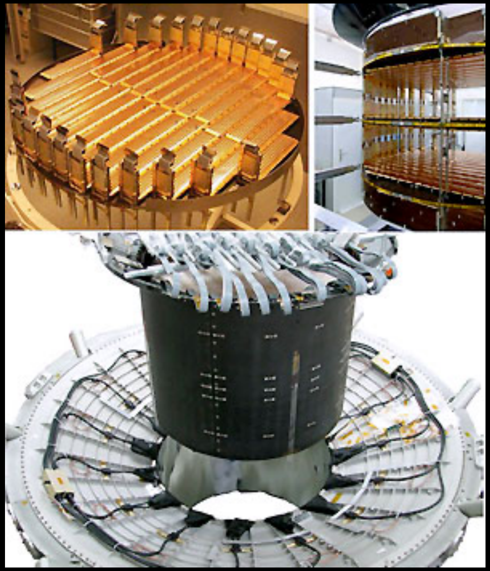

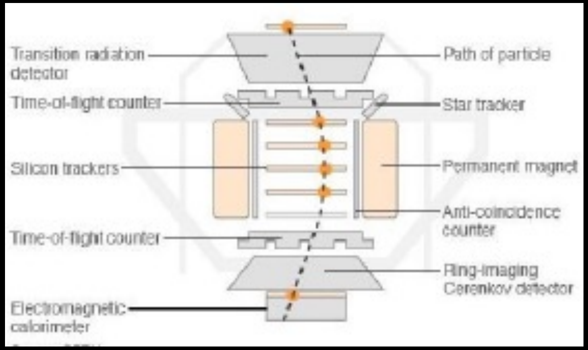

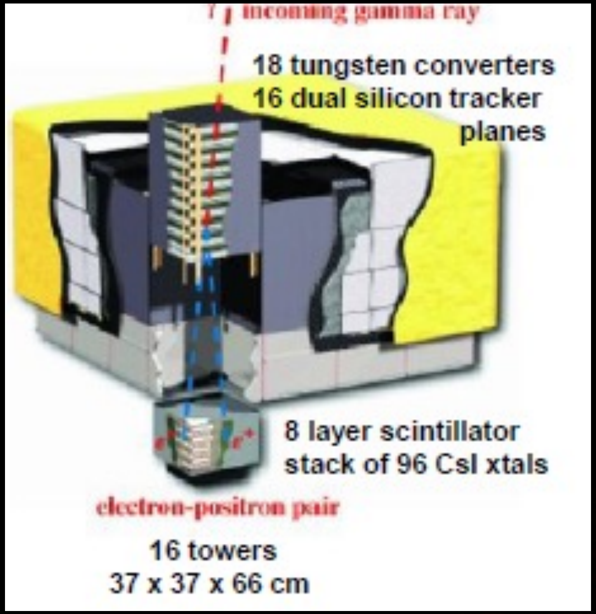

FERMI Large Area Telescope

Gamma-ray detector

Cycle of pulsed gamma rays from the Vela pulsar. Constructed from photons detected by Fermi's Large Area Telescope.

Roger Romani

….Ground Detectors – Cosmic Rays

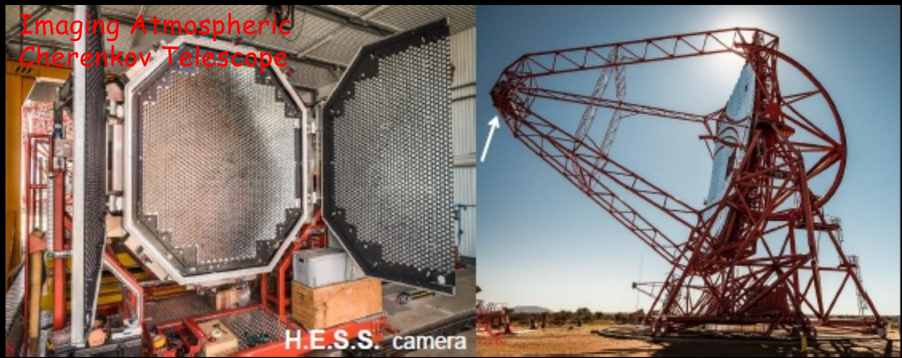

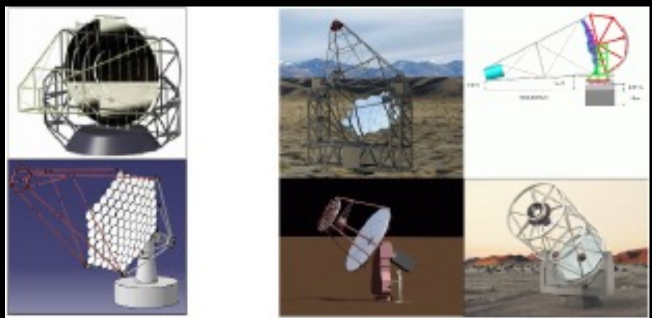

SST 70x (S) : > few TeV
>5 m^2, >8° FoV, <0.25° pxl

MST 25x (S) : 0.2-10 TeV
>88 m^2, >7° FoV, <0.18° pxl

LST 4x (S) : 20 GeV - 1 TeV
>330m^2, >4.4° FoV, <0.11° pxl size

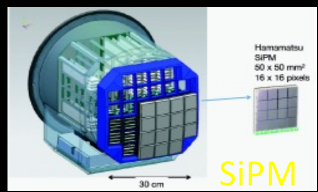

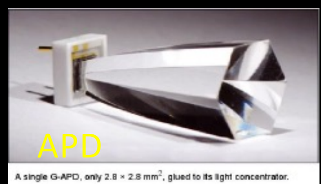

Camera Options

Pierre Auger Observatory

UHE 10^{20}eV
1600 water Cherencov detectors

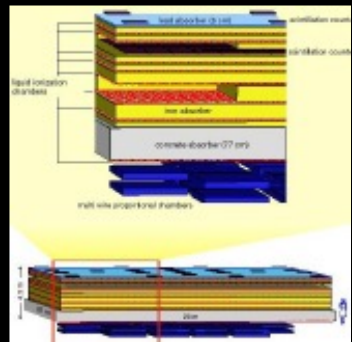

KASCADE-Grande

200x200 m^2 scint. array
20x16 m^2 h. calorimeter
128 m^2 muon tracker

ARGO-YBJ -RPCs

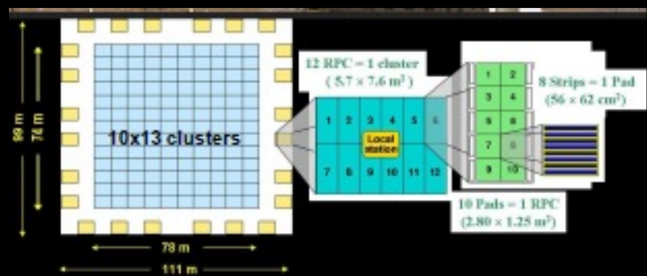

Follow-up project LHAASO

…… ICE-Cube (South Pole Neutrino Experiment)

Digital Optical Boards (DOMs) are deployed on 86 "strings" of 60 modules each at depths ranging from 1,450 to 2,450 meters

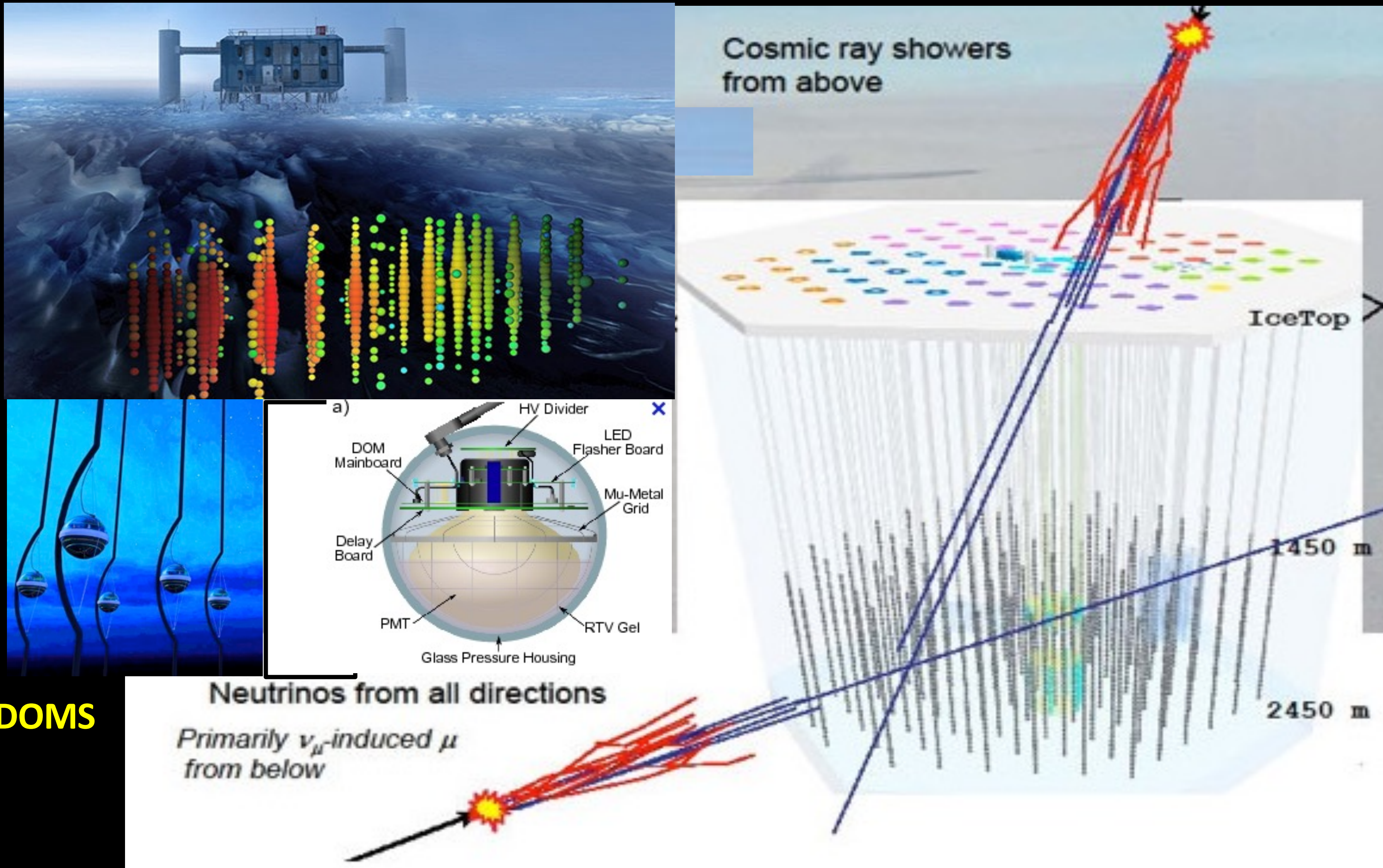

DOMS

……. Environmental Radiation Monitoring

Gamma Dose Rate (GDR) networks in Europe

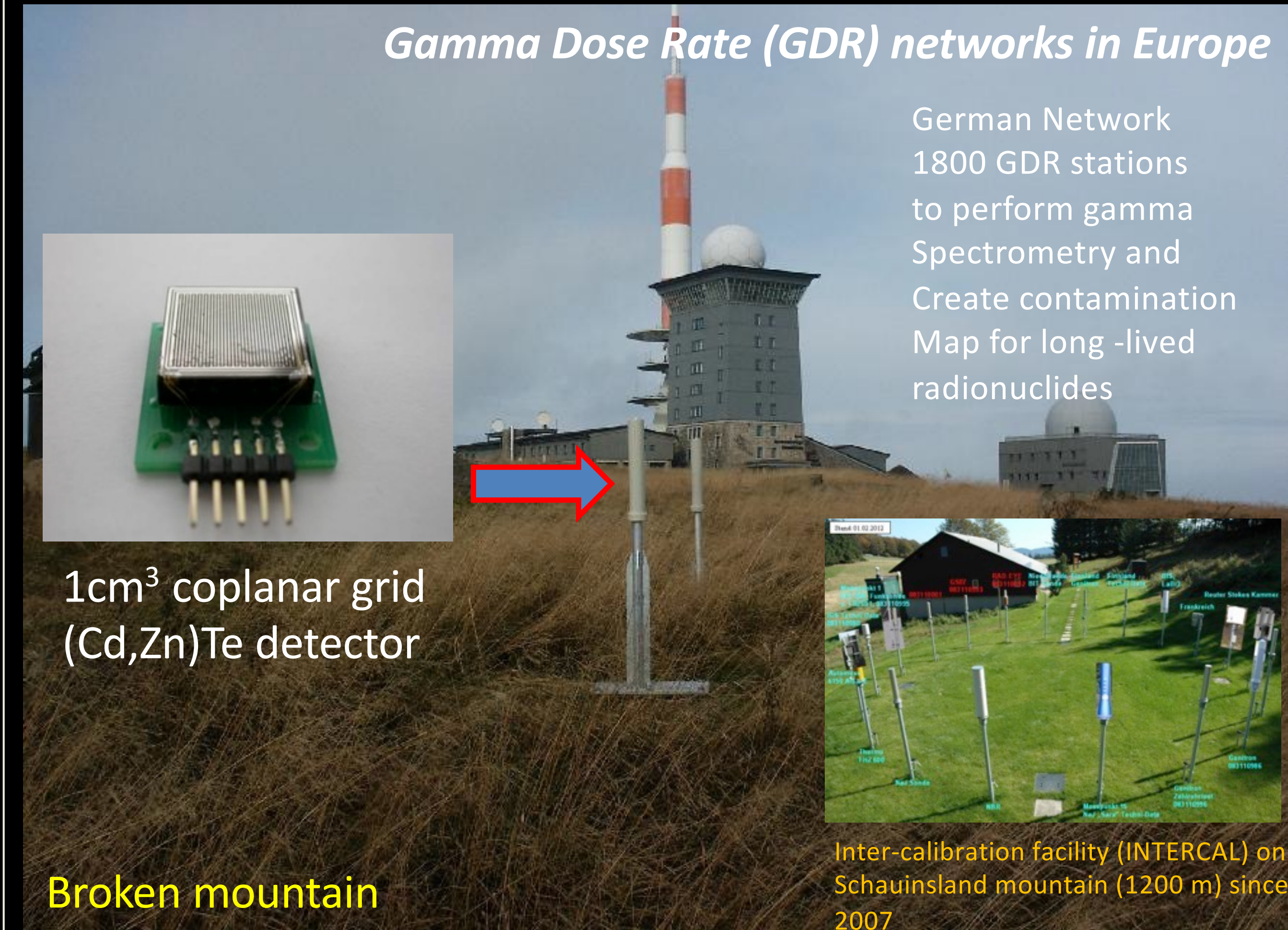

German Network
1800 GDR stations
to perform gamma
Spectrometry and
Create contamination
Map for long -lived
radionuclides

1cm^3 coplanar grid
(Cd,Zn)Te detector

Broken mountain

Inter-calibration facility (INTERCAL) on Schauinsland mountain (1200 m) since 2007

European countries established GDR networks during the cold war period and improved these networks after the Chernobyl accident in 1986.

Monitoring of:

nuclear facilities
atomic bomb scenarios
terroristic attacs

U. Stöhlker

X-ray energy of the most common medical and biological applications

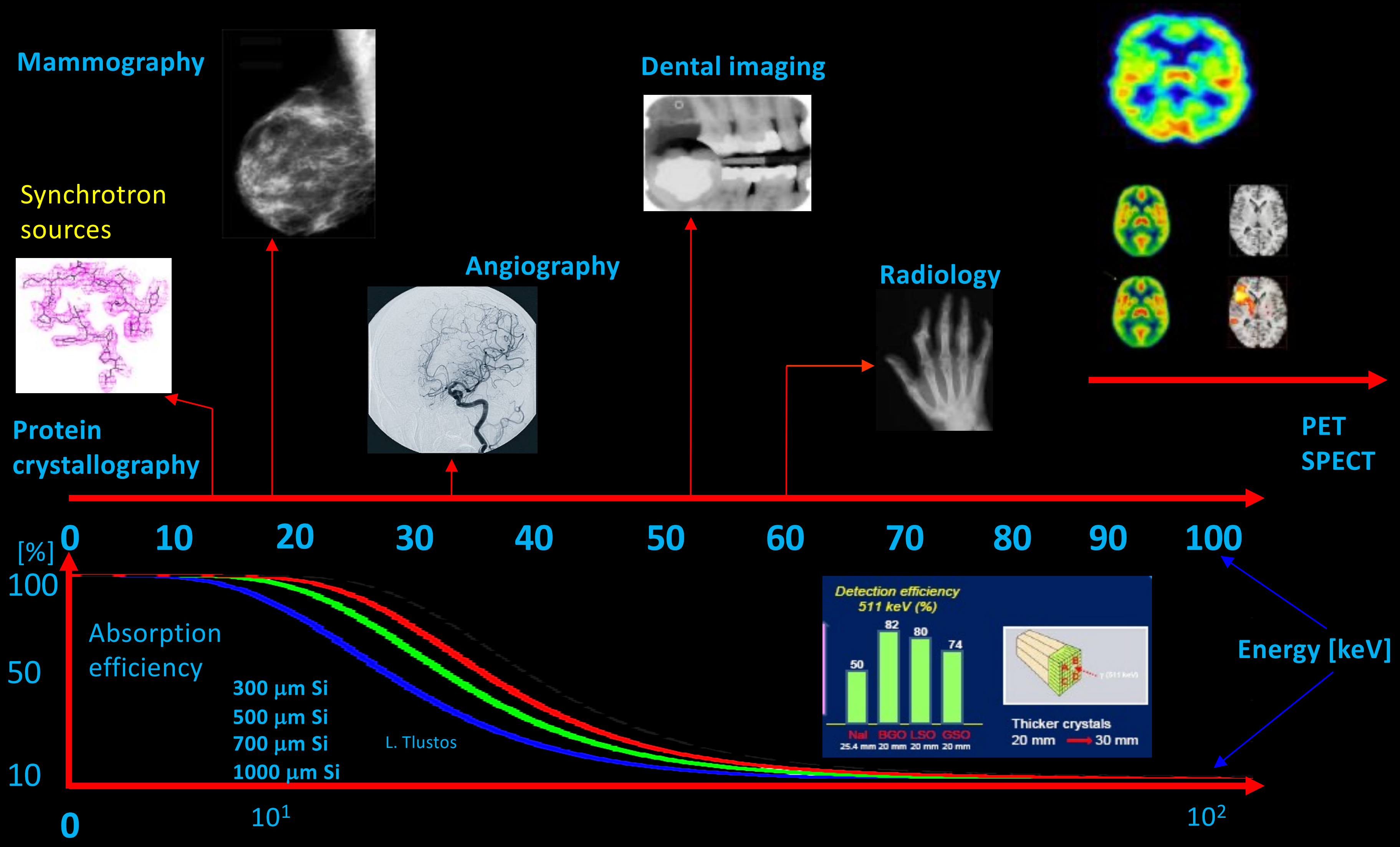

Cinzia Da Via, Stony Brook USA and The University of Manchester, UK– 2022

C. Da Via' 2007

Direct / indirect conversion

The target is to reduce the dose to the patient!

Scintillator
Gadox, YAG CsI
(high Z)

Photodiode/ CCD

electronics

electronics

Sampled image

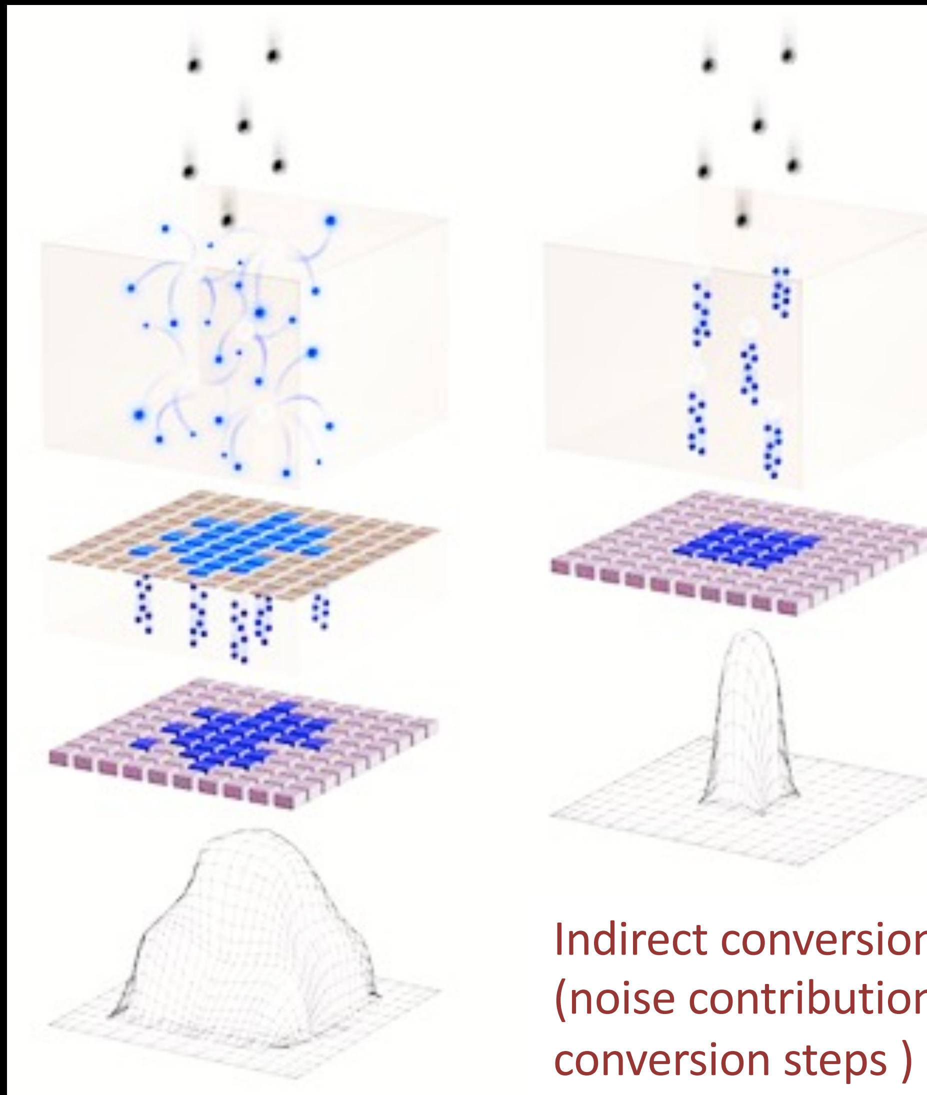

X-rays

Direct conversion
Si, Ge, CdTe,
GaAs, Se

Sampled image

Indirect conversion implies lower DQE (noise contribution from the two conversion steps)

High Z semiconductors: CdTe and CdZnTe

Taka Tanaka (SLAC/KIPAC)

- High detection efficiency
- Poly-crystalline material
- Poor uniformity
- Very high resistivity (semi-insulating)
- Low leakage current

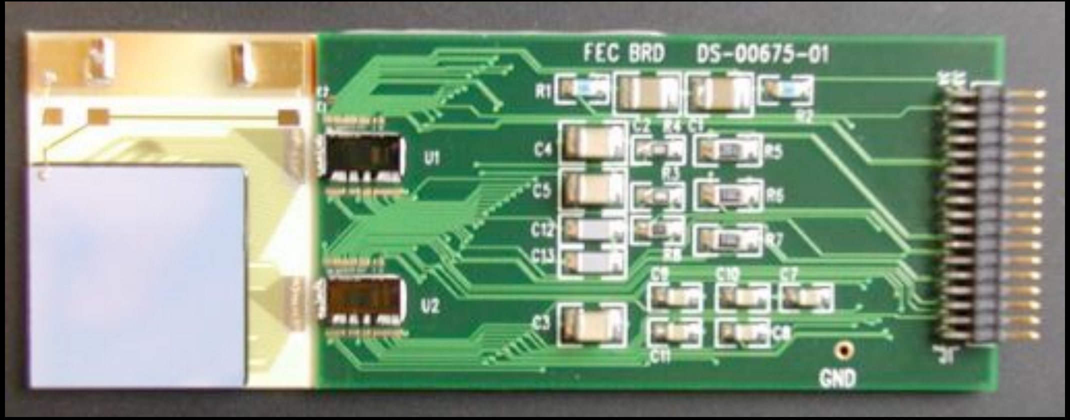

area: 18 " 18 mm2
thickness: 0.5 mm
pixel size: 2 " 2 mm2,
64 ch, cathode side
guard ring: 1 mm width

Fabricated at IDEAS Norway

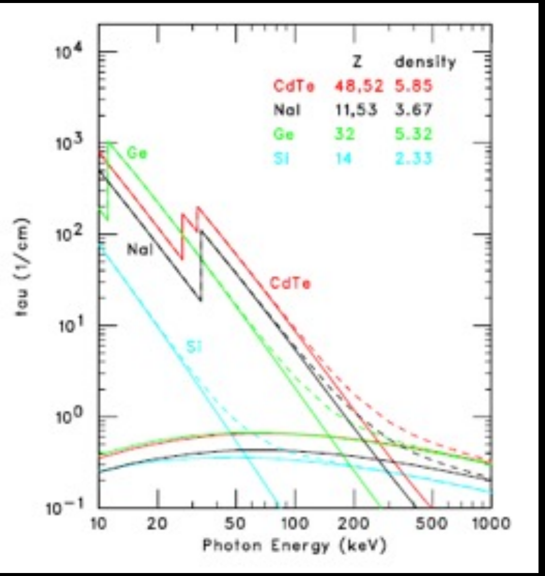

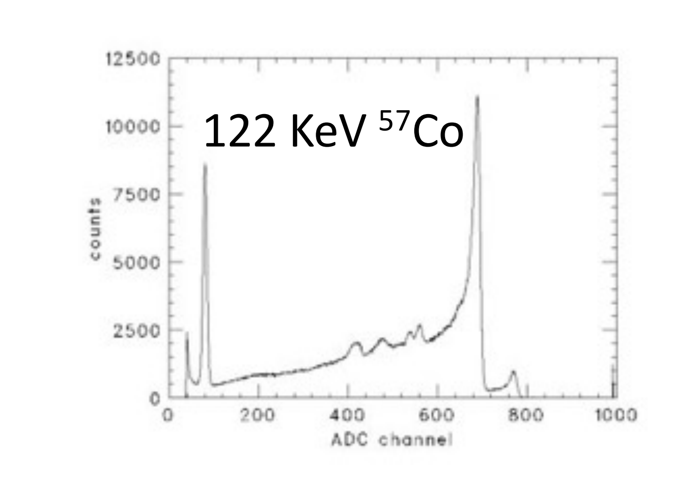

Indirect Conversion: Scintillators and Silicon Photomultipliers (SiPm, GM-APD, MPPC…)

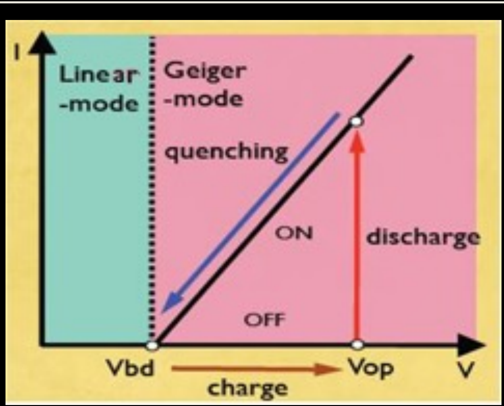

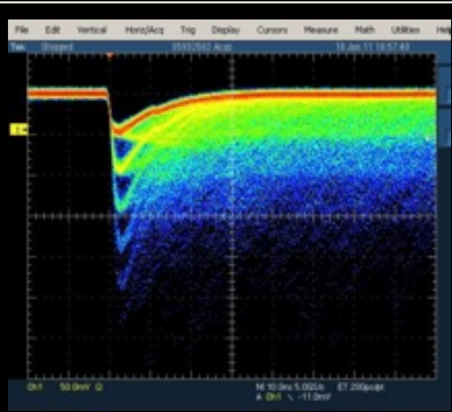

1 pixel
2 pixels
3 pixels

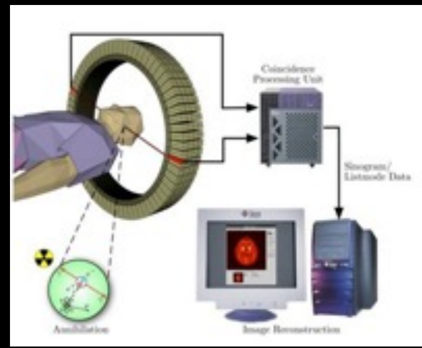

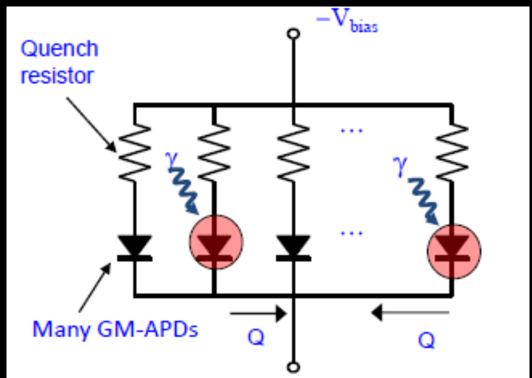

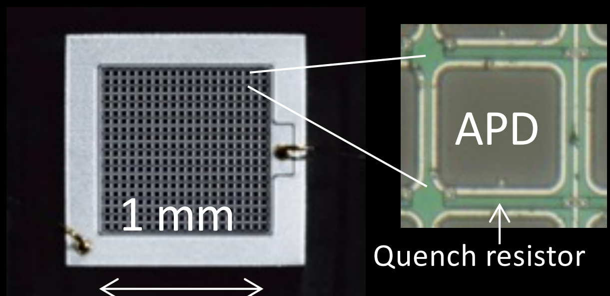

- SiPm requires a special doping profile to allow a high internal field (>10^5 V/cm) which generates avalanche multiplication
- APD cell operates in Geiger mode (= full discharge), however with (passive/active) **quenching**.
- The avalanche formation is intrinsically very fast (100ps), because confined to a small space.
- High Gain G ~ 10^5 -10^6 at rel. low bias voltage (<100 V)
- G is Sensitive to temperature and voltage variations
- Fill factor still low due to quench resistor on the surface (but work in progress to solve this)

Applications in PET

coincidence of two 511 keV photons define a line of record.

•Take projections under all angles

•(2/3D) Tomographic reconstruct of data

Cinzia Da Via, Stony Brook USA and The University of Manchester, UK– 2022

SiPm Commercial Activity

From C. Joram CERN

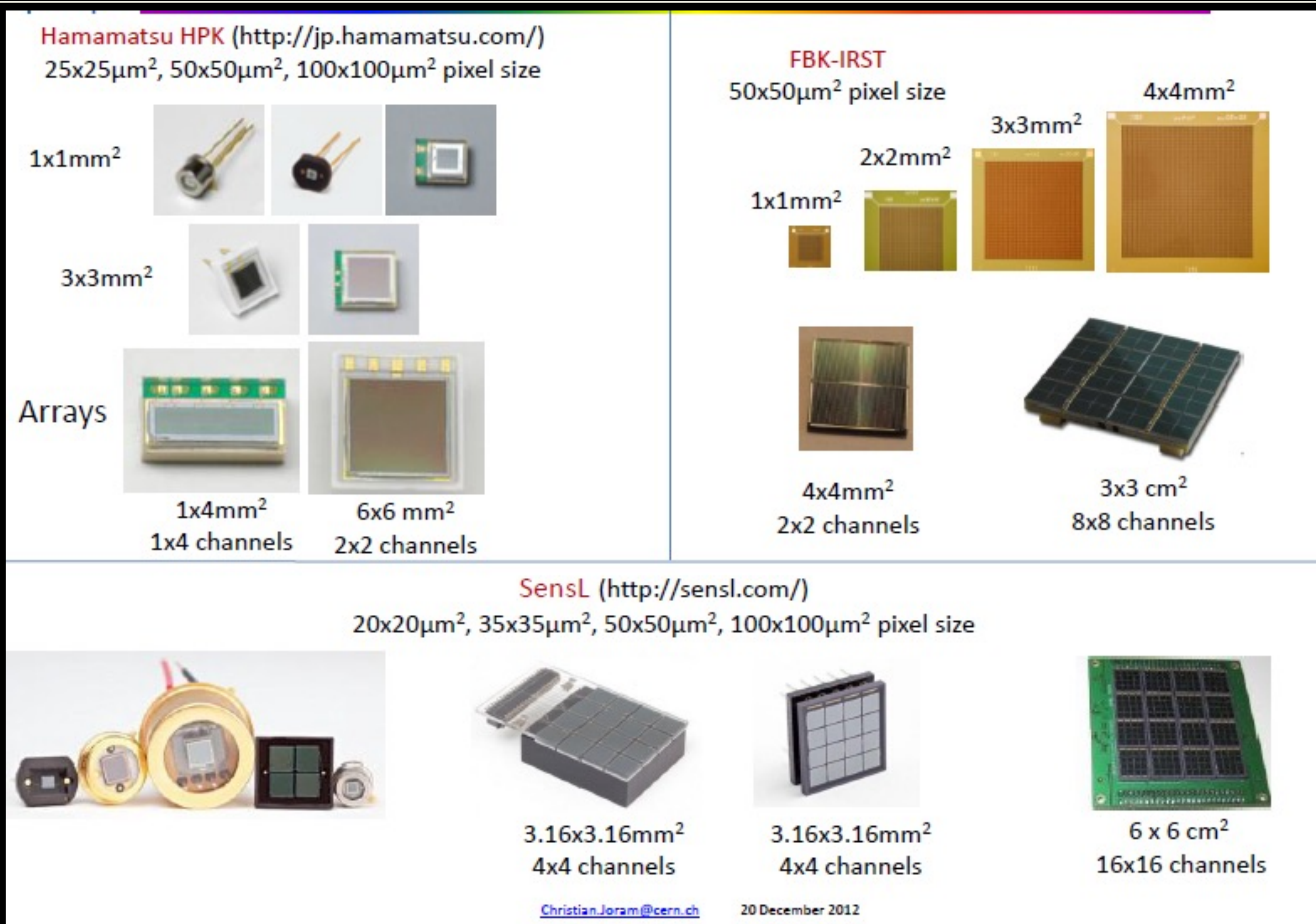

Overview of commonly used scintillators

Scintillators for PET

	1962	1977	1995	1999	2001	2003	2007
	NaI	BGO	GSO:Ce	LSO:Ce	LuAP:Ce	$LaBr_3$:Ce	LuAG:Ce
Density (g/cm^3)	3.67	7.13	6.71	7.40	8.34	5.29	6.73
Atomic number	51	75	59	66	65	47	63
Photofraction	0.17	0.35	0.25	0.32	0.30	0.13	0.30
Decay time (ns)	230	300	30-60	35-45	17	18	60
Light output (hν/MeV)	43000	8200	12500	27000	11400	70000	>25000
Peak emission (nm)	415	480	430	420	365	356	535
Refraction index	1.85	2.15	1.85	1.82	1.97	1.88	1.84

Digital radiography with gas based MWPC in the 1970ies

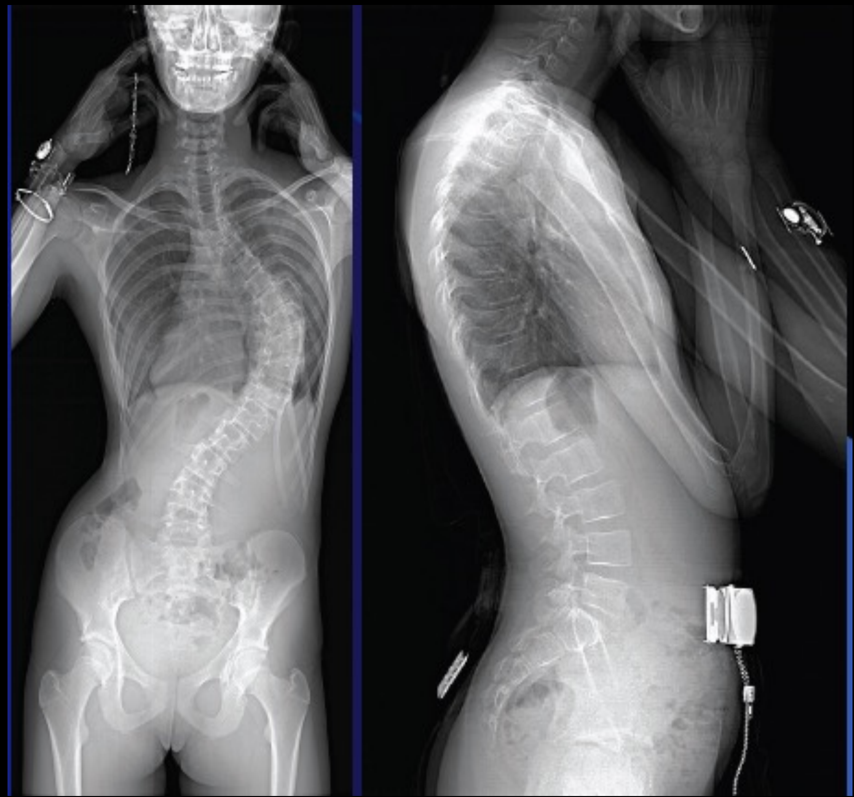

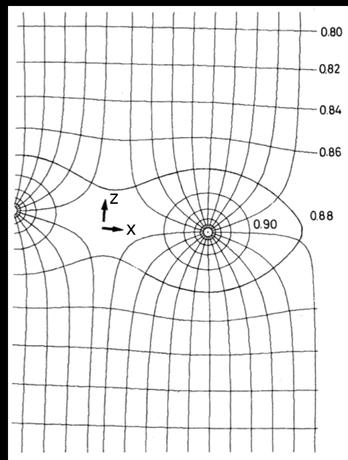

with 10 time less dose than traditional radiographic film!

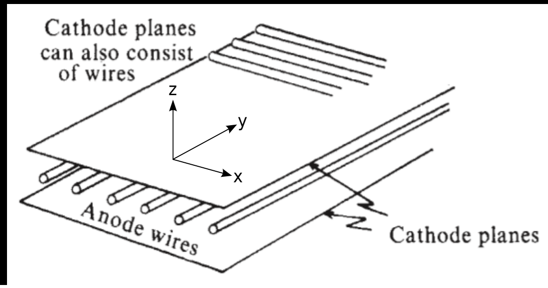

Cinzia Da Via, Stony Brook USA and The University of Manchester, UK– 2022

Nuclear Medicine: Positron Emission Tomography

Sign the degree of activity of an organ hungry of glucose ---> show abnormal glucose metabolism like cancer tumour cells

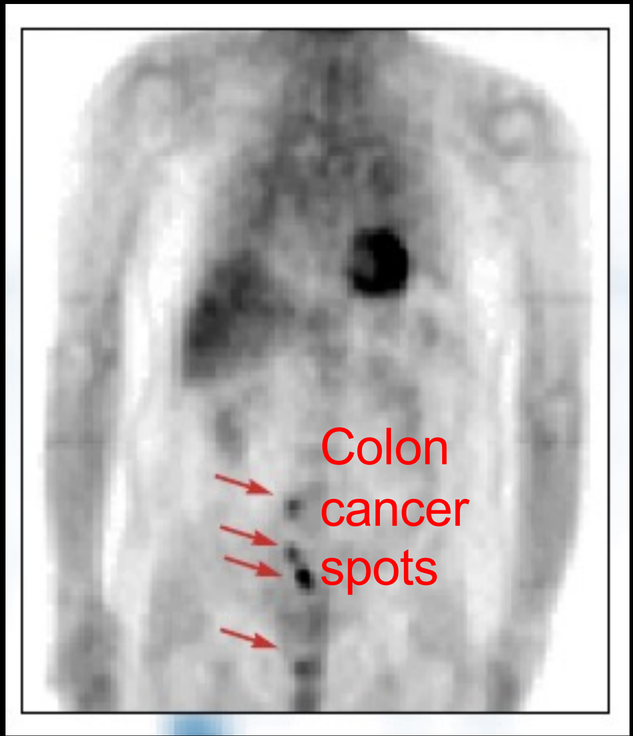

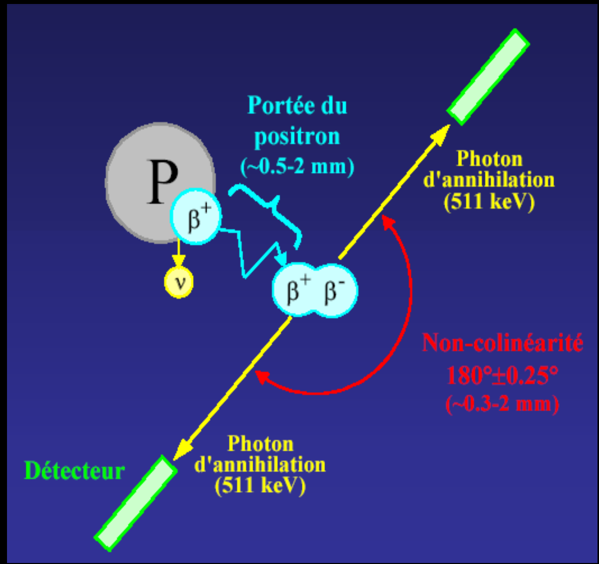

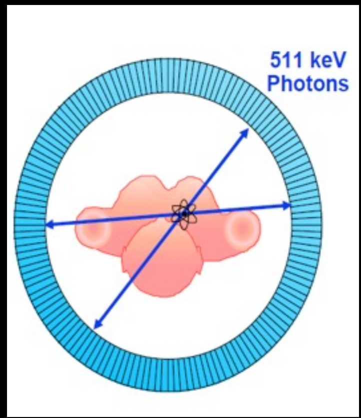

Cinzia Da Via, Stony Brook USA and The University of Manchester, UK– 2022

Direct conversion Synchrotron Radiation: Protein crystallography 12 KeV

Cinzia Da Via, Stony Brook USA and The University of Manchester, UK– 2022

X-rays

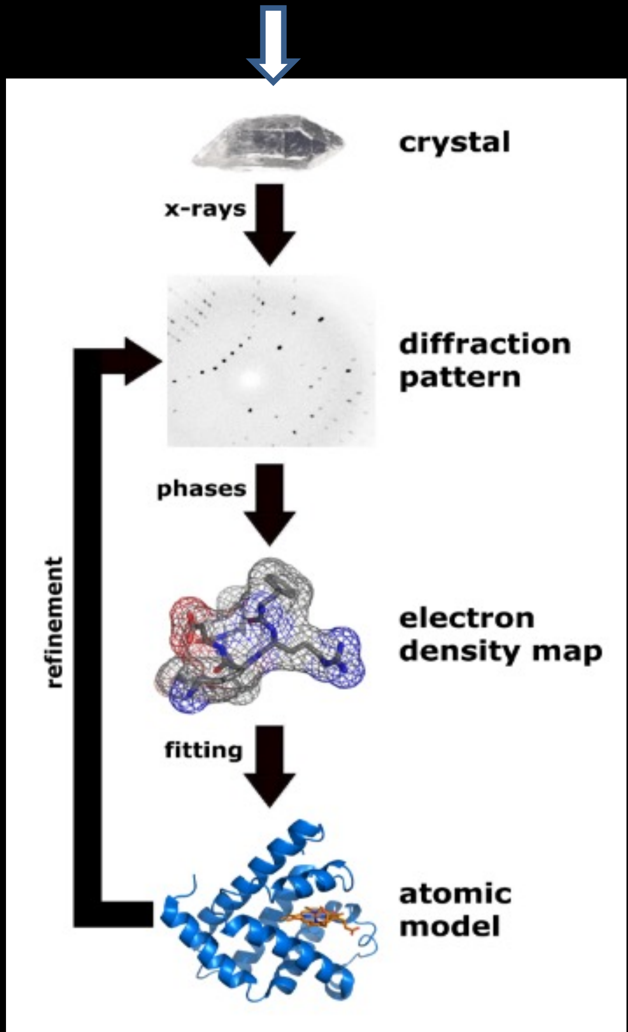

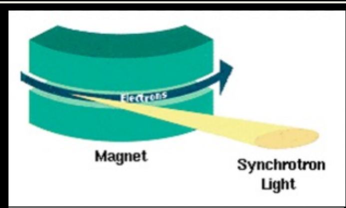

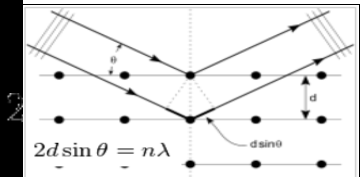

Bragg Law

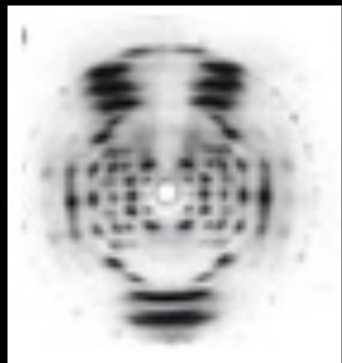

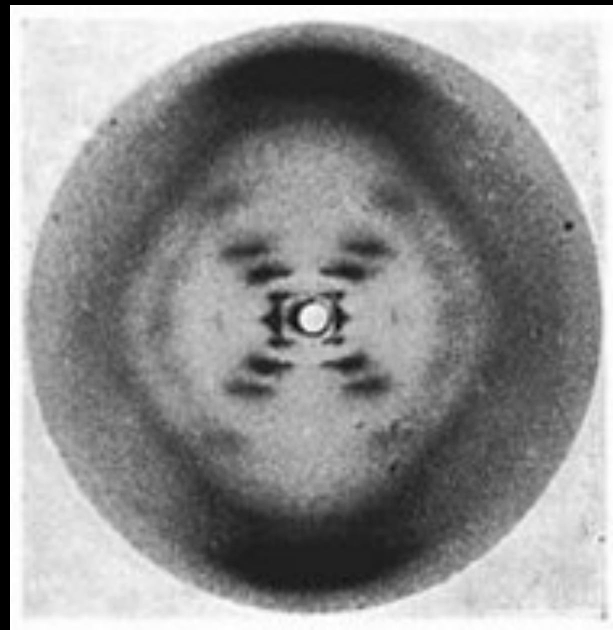

X-ray diffracted Photographic image of the double helix taken in 1952 by Rosalind Franklin and Raymond Gosling. The DNA sample was fibrous DNA

Some of the existing electronics chips for medical –synchrotron

Single photon Counting | Charge Integration

Medipix2 Quad
Pixels: 512 x 512
Pixel size: 55 x 55 mm^2
Area: 3 x 3 cm^2

Medipix

pixellated detector (Si, GaAs, CdTe, 3D thickness: 300/700/1000mm

Gotthard

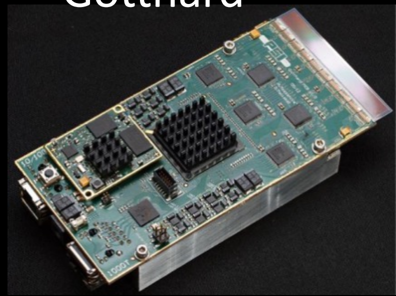

AGIPD

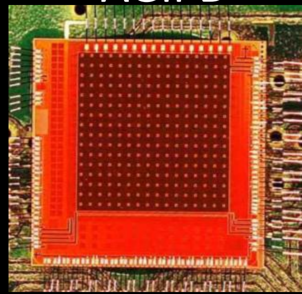

Mithen II

Eiger

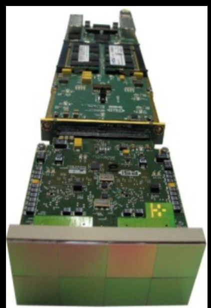

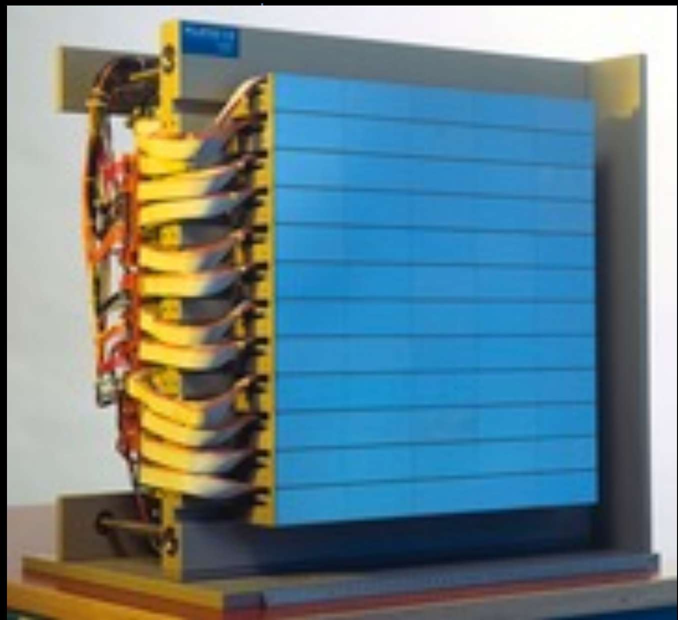

The PILATUS 6M,

424 x 435 mm2 with 170 × 170 μm^2 (2463 x 2527) 6 million pixels, has been developed at PSI and commercialized by the company Dectris for synchrotron imaging

The challenge of The CERN Large Hadron Collider (LHC)

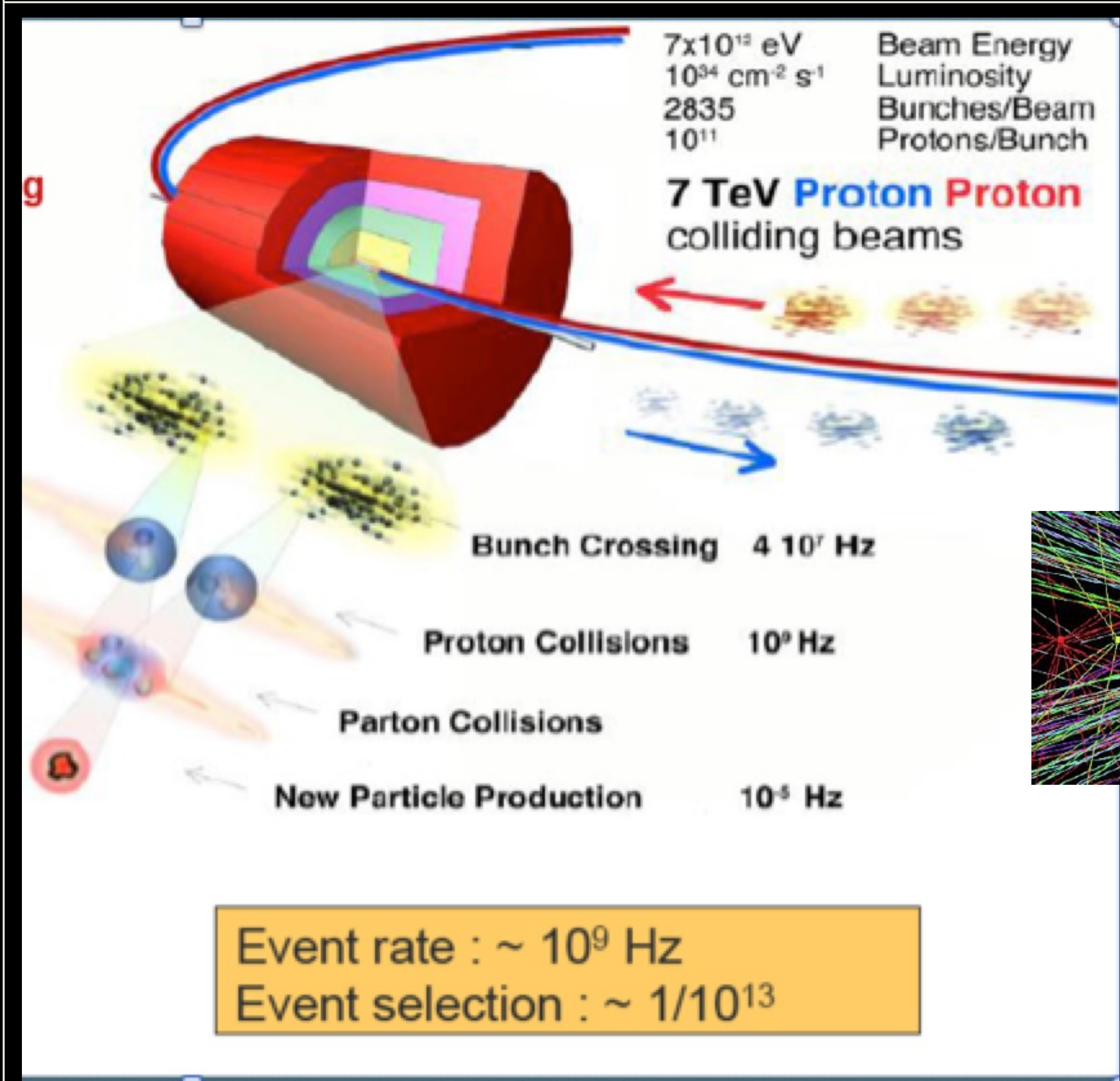

A microscope to observe Dimensions as small as 10^{-17}m!

Collisions every 25 ns

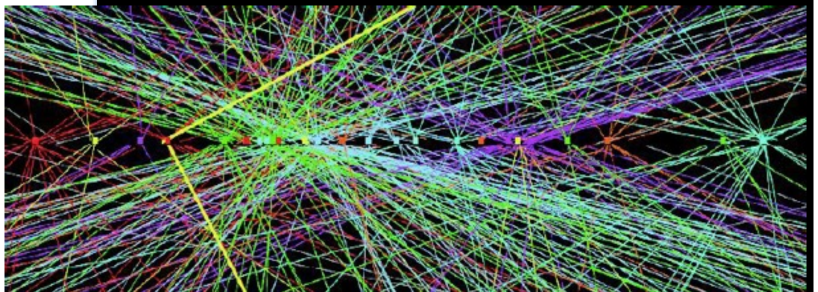

Z -> μμ event at LHC ATLAS 15 April 2012

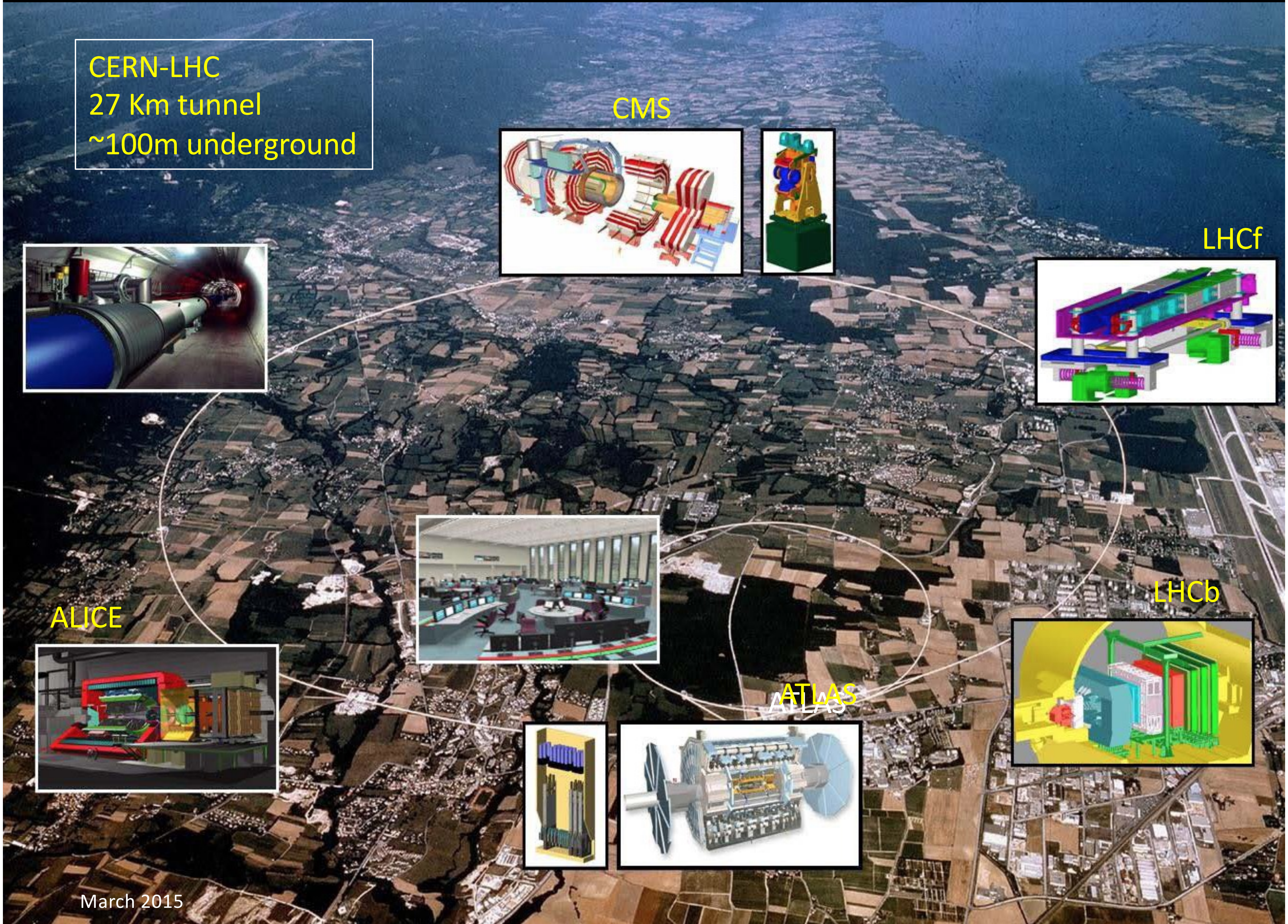
CERN-LHC
27 Km tunnel
~100m underground
CMS
LHCf
ALICE
LHCb
ATLAS
March 2015

A typical particle detector: CMS

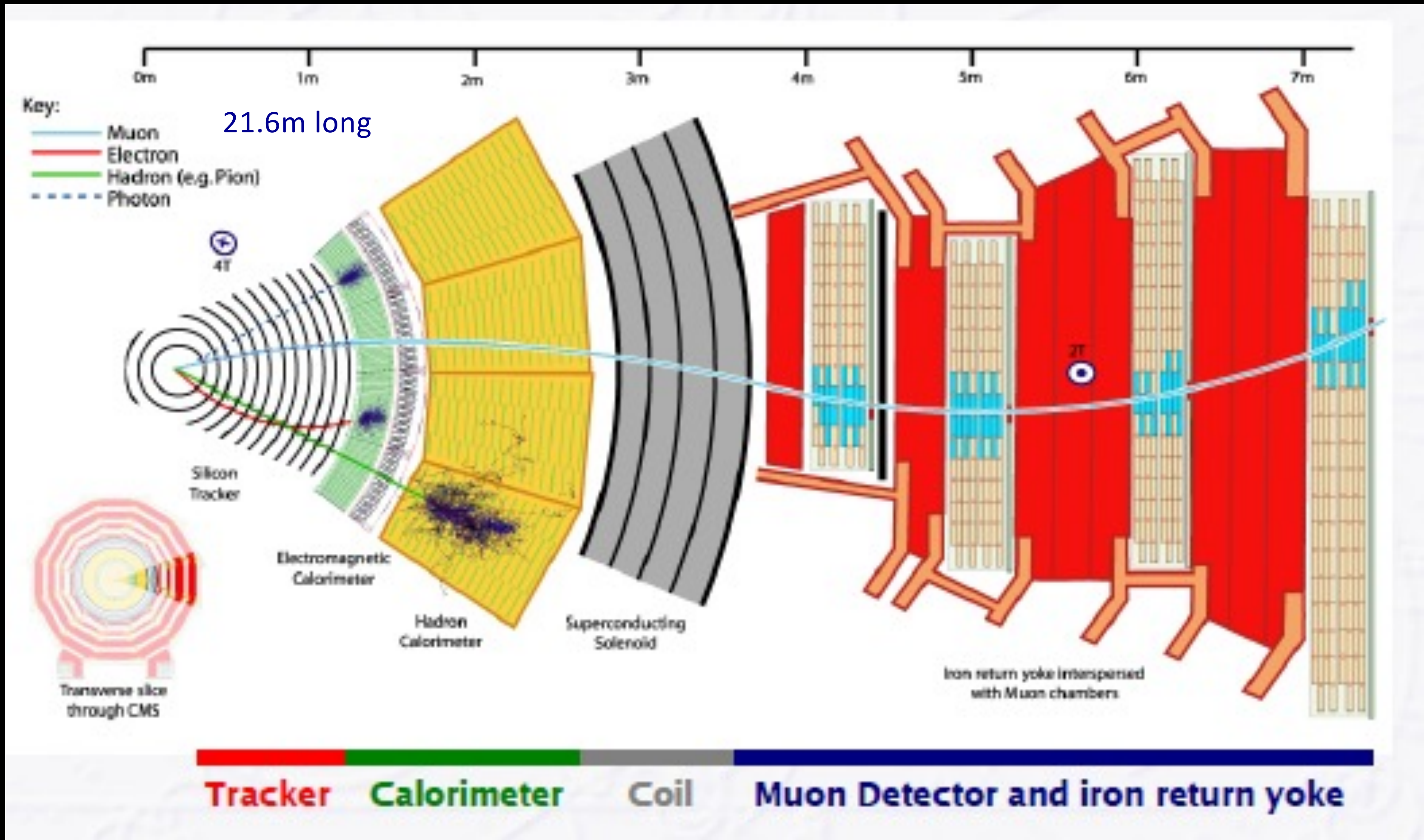

ATLAS and CMS use alone more that 250m^2 of Silicon Strips to “image” charged particles

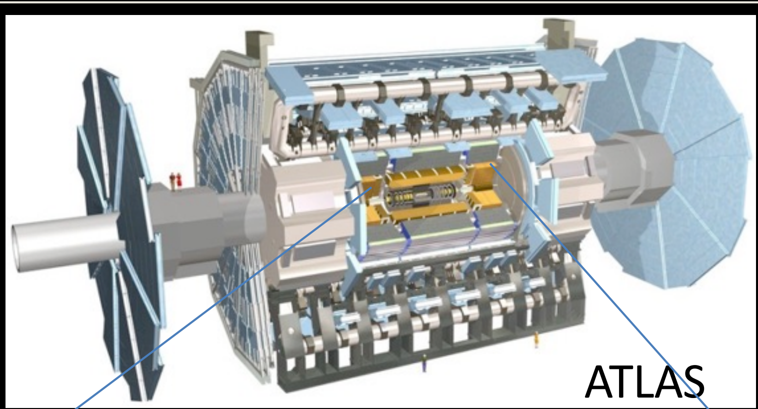

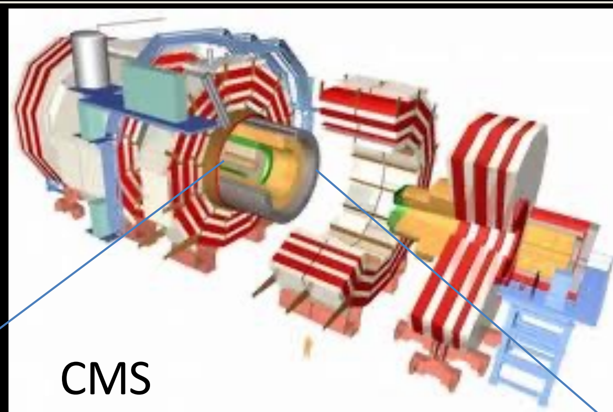

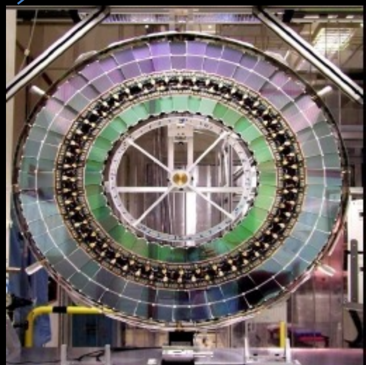

Strips
61m^2 of silicon.
6.2million channels 4 barrel layers + 9 disks per endcap
30cm < R < 52cm

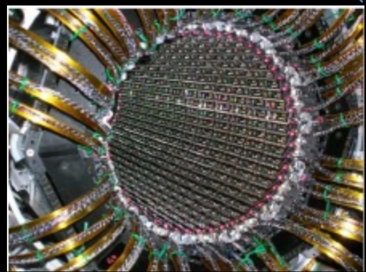

Pixels
3 Barrel layers (r=5,9,12 cm)
2 end caps each with 3 disks
80Mpixels
50x400um2
Digital I/O

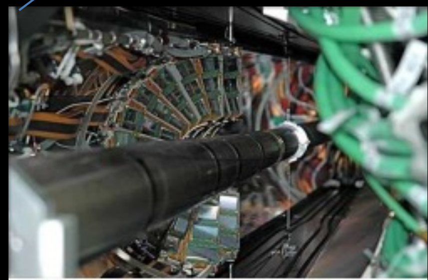

Pixels
3 barrel layers
2 end caps each with 2 disks
66 Mpixels 150 x 100um2
Analog I/O

Strips
198 m^2 of silicon,
9.3 million channels
Inner : 4 barrel layers,
3 end-cap disks
Outer: 6 barrel layers,
9 weels
22cm < R < 120cm

The current LHC environment for pixel detectors

- Pixels and Strips are immersed is a multiple-particle environment
- Radiation decrease radially from the beam
- Several vertices to identify

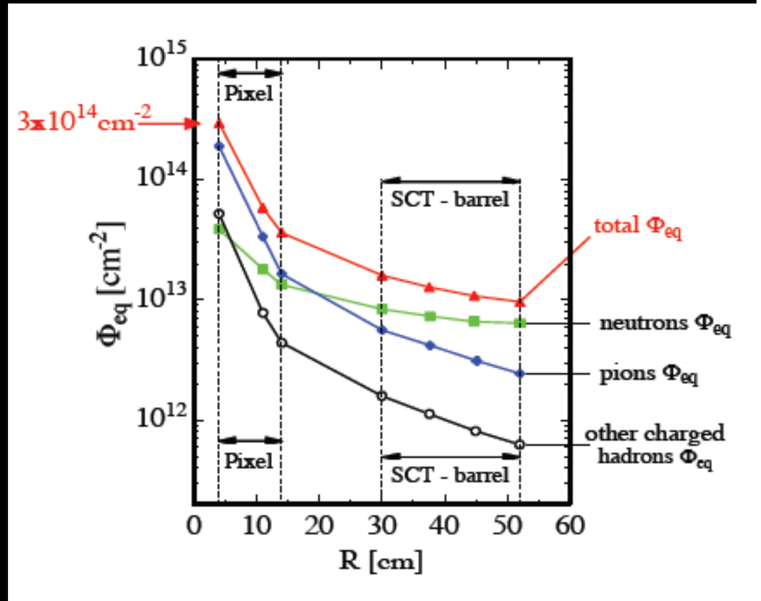

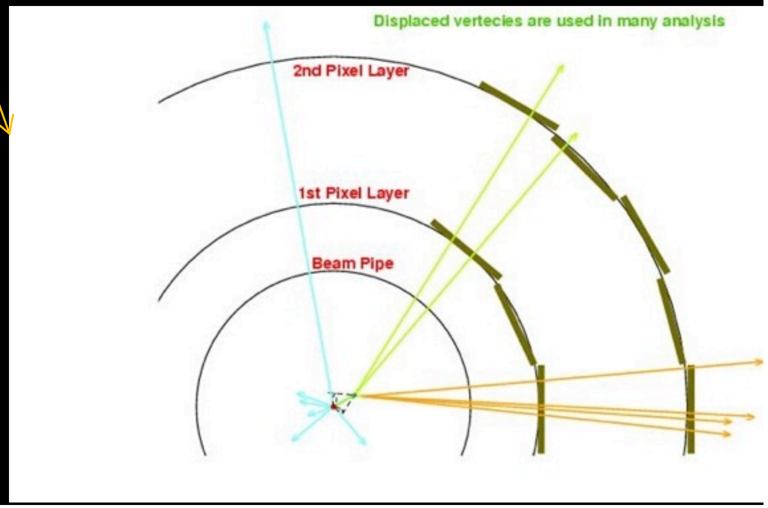

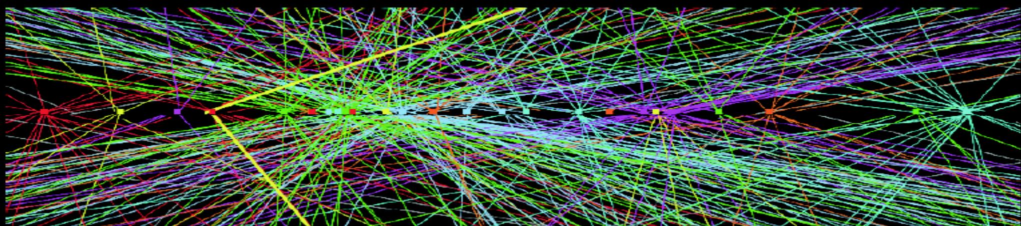

What happens during irradiation to silicon detectors?

Defects formation in irradiated silicon

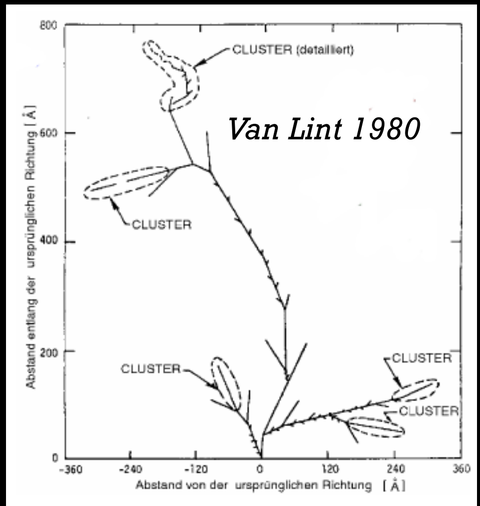

Primary Knock on Atom

Displacement thresholds in Si:
Frenkel pair E~25eV
Defect cluster E~5keV
For X-Rays E~250KeV

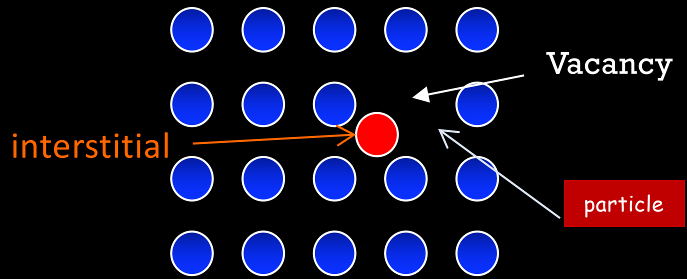

V,I MIGRATE UNTIL THEY MEET IMPURITIES AND DOPANTS TO FORM STABLE DEFECTS

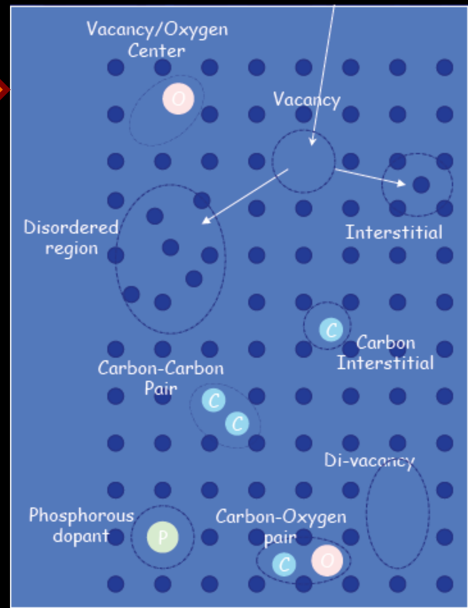

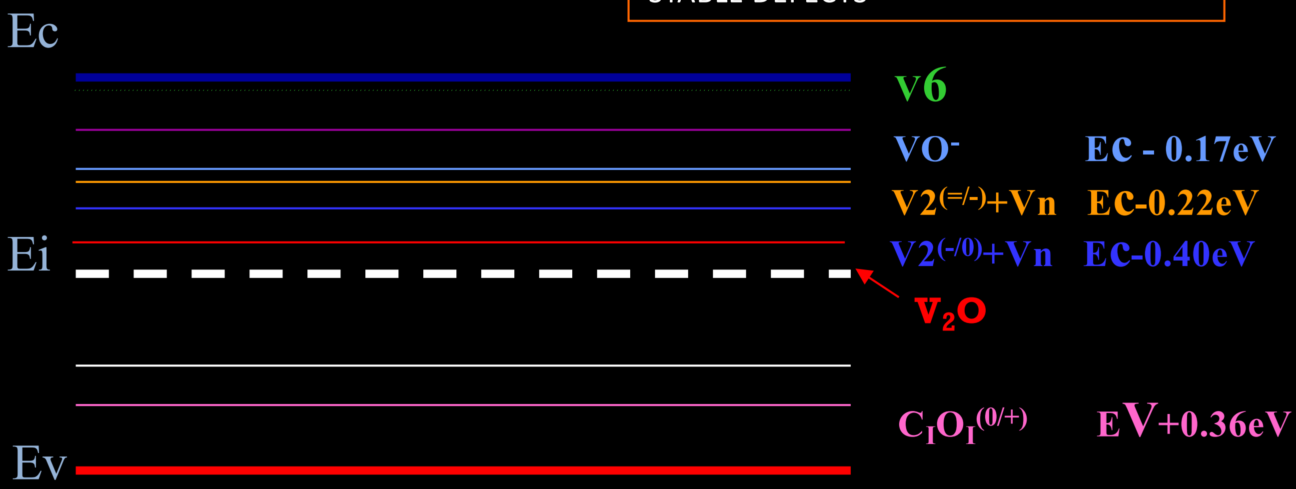

Defects position in the bandgap

Pixels Sensors trends for the next tracking detectors

Radiation Hardness hybrid ⟵ ⟶ Granularity, low mass monolithic

3D sensors

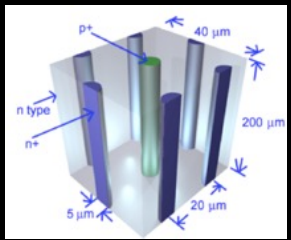

diamond

n-in-n, n-in-p-
planar

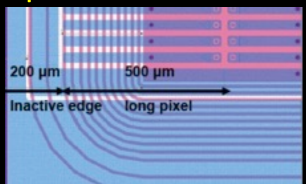

CCD

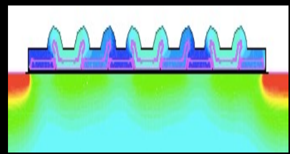

DEPFET

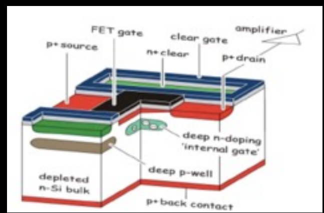

SOI

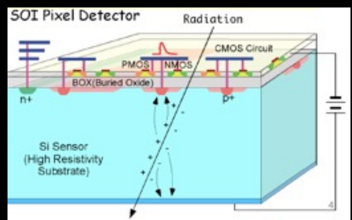

Mimosa

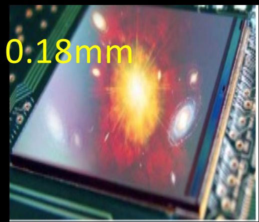

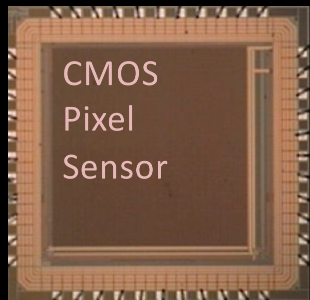

INMAPS

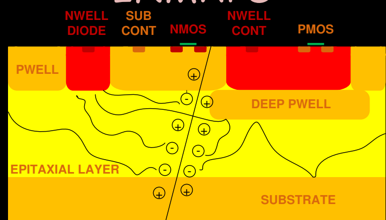

HV-MAPS

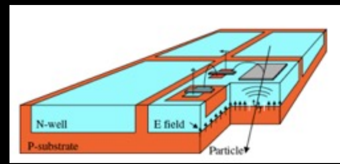

deepNwell

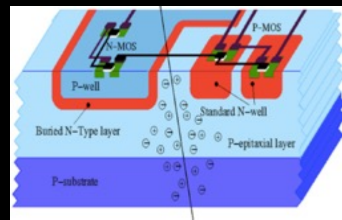

LePiX

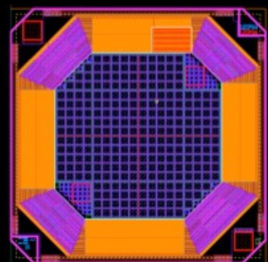

3D radiation sensors

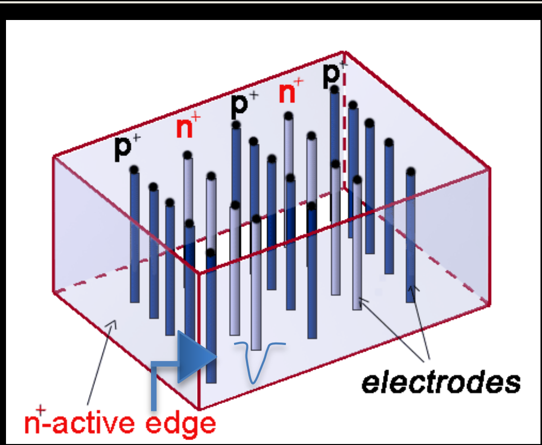

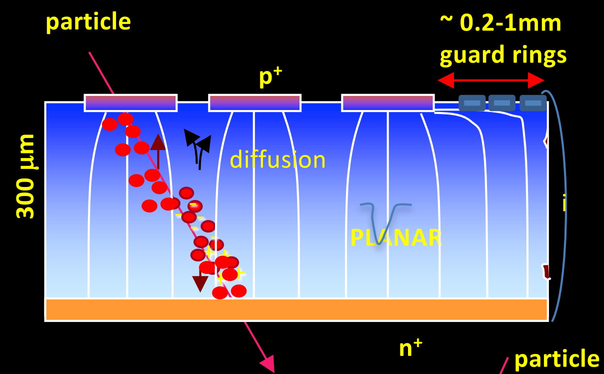

V=70V
Before
irradiation

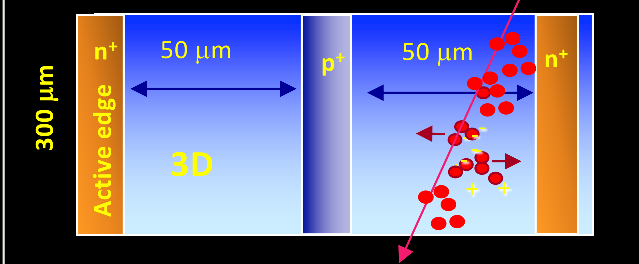

V=7V
Before
irradiation

Drift lines parallel to the surface

3D silicon detectors were proposed in 1995 by S. Parker, and active edges in 1997 by C. Kenney.

Combine traditional electronics processing and MEMS (Micro Electro Mechanical Systems) technology.

Electrodes are processed inside the detector bulk instead of being implanted on the Wafer's surface.

The edge is an electrode! Dead volume at the Edge < 5 microns!

The electric field is parallel to wafer's surface: and smaller inter-electrode spacing: low bias voltage, low power, reduced charge sharing and high speed – for the same wafer thickness

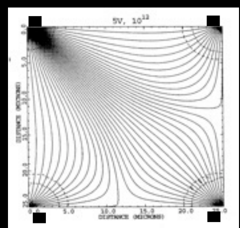

MEDICI simulation
of a 3D structure

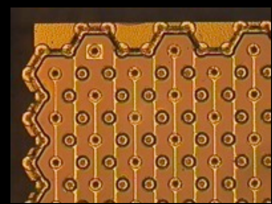

3D is “geometrically” radiation hard at low V_{bias}

Ramo’s theorem

$$\lambda = v_D \cdot \tau$$

$$S = \frac{\lambda}{L}\left[1 - \exp(-\frac{x}{\lambda})\right]$$

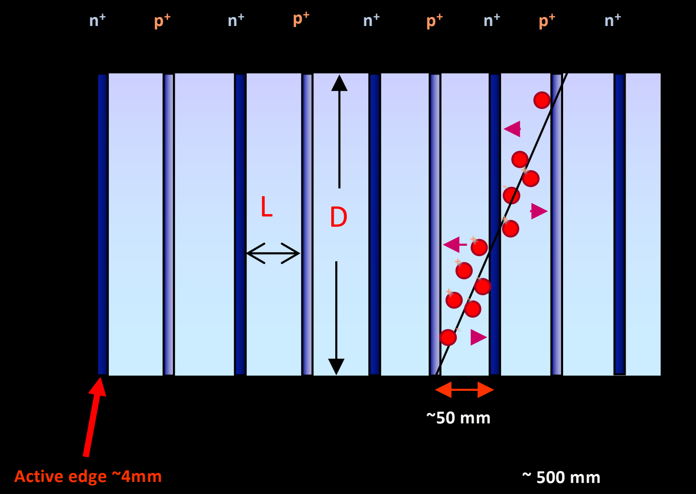

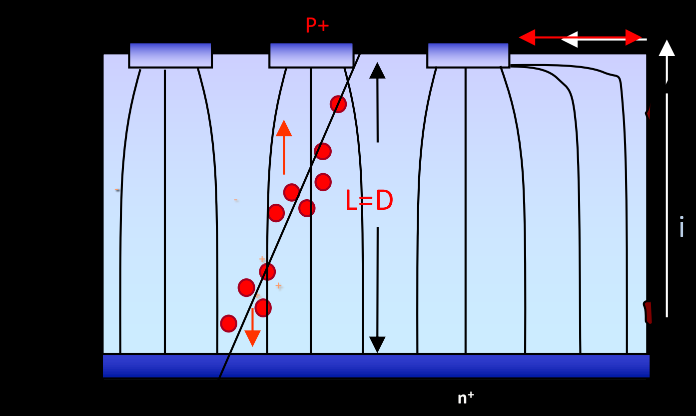

PLANAR

3D 4E
3D 3E
3D 2E
Diamond
Thick Si
Thin Si

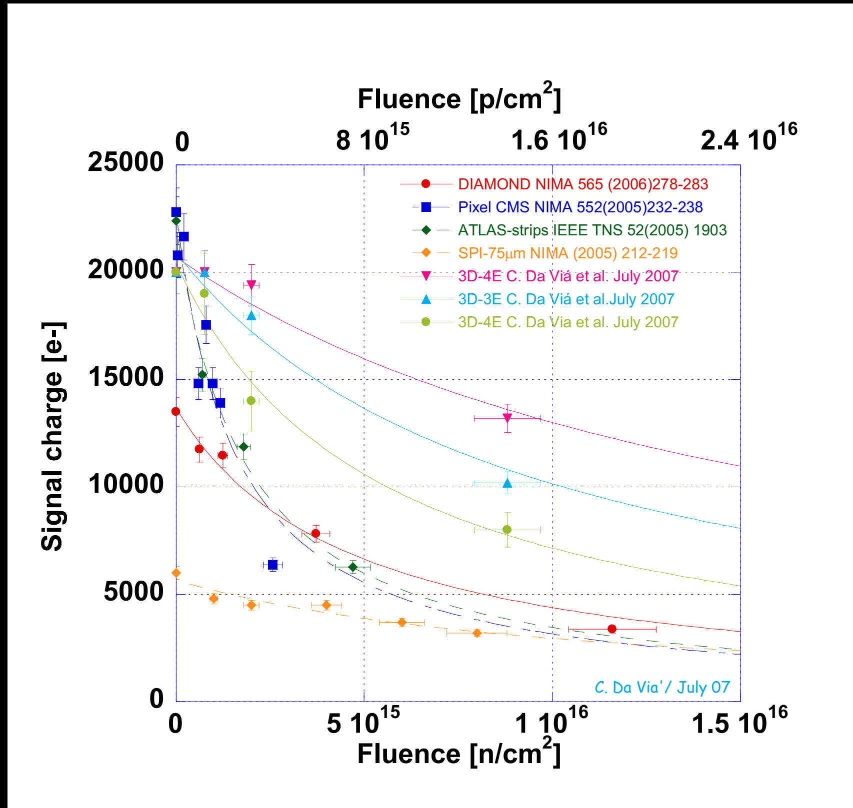

NIM A 603 (2009) 319–324

3D sensors are now in the core of ATLAS at CERN LHC

3DATLAS R&D Collaboration

NIMA 694 (2012) 321–330
2012 JINST 7 P11010.

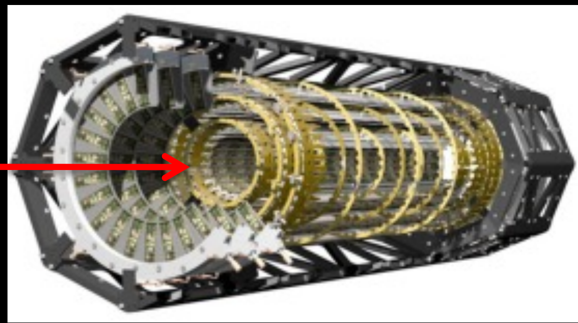

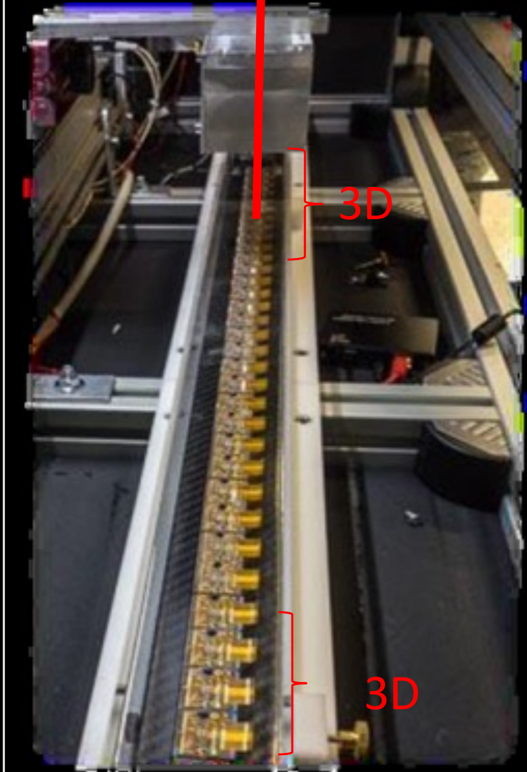

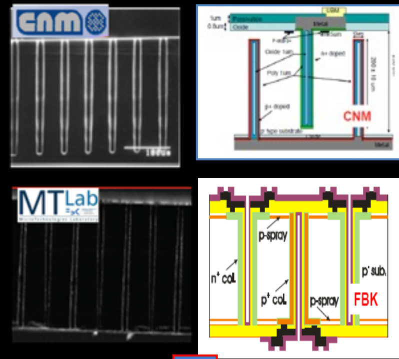

3D sensors just being installed in the first LHC detector upgrade in the ATLAS – Insertable B-Layer (IBL)

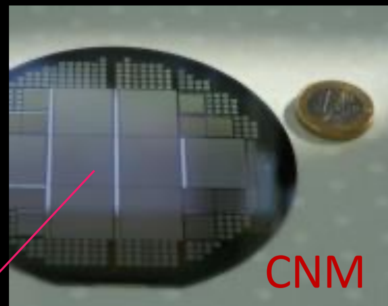

>300 sensors fabricated to cover 25% IBL

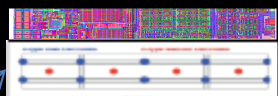

250 x 50 um^2

FE-I4 = 2x2cm^2
336 x 80
250x50um^2,
26880 pixels

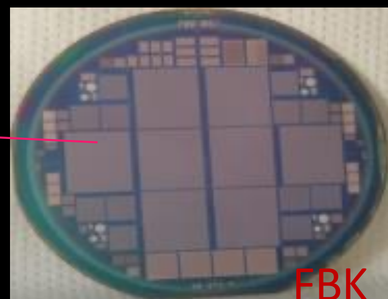

Cinzia Da Via, Stony Brook USA and The University of Manchester, UK– 2022

3D Vertically Integrated Module with CO2 internal cooling

C. Da Via, F. Munoz-Sanchez, N. Dann,
D. Hellesmidht, P. Petagna, G. Romagnoli

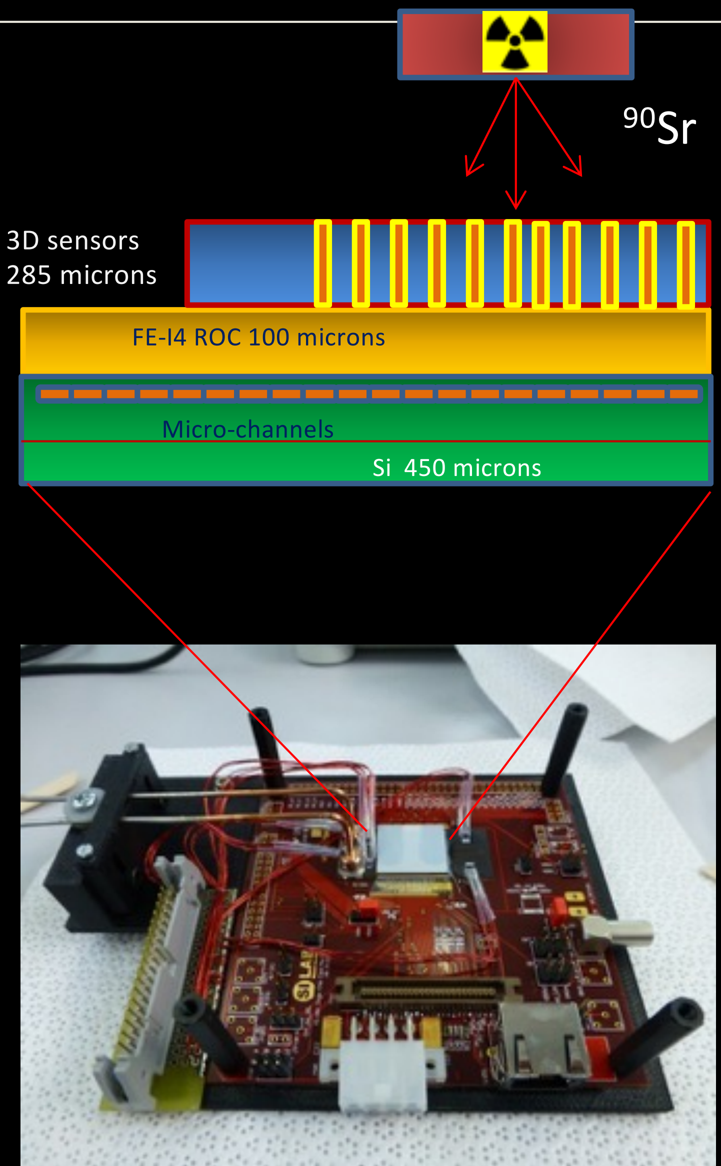

- 3D silicon : CNM double side 285 um thick IBL qualification batch
- FE-I4A: thinned to 100um at IZM
- Si-Si micro-channels
  designed by CERN PH-DT,
  produced by PH-DT in EPFL CMi cleanroom,
  direct bonding CSEM
- Glue: 2-components
  Masterbond EP37-3FLFAO

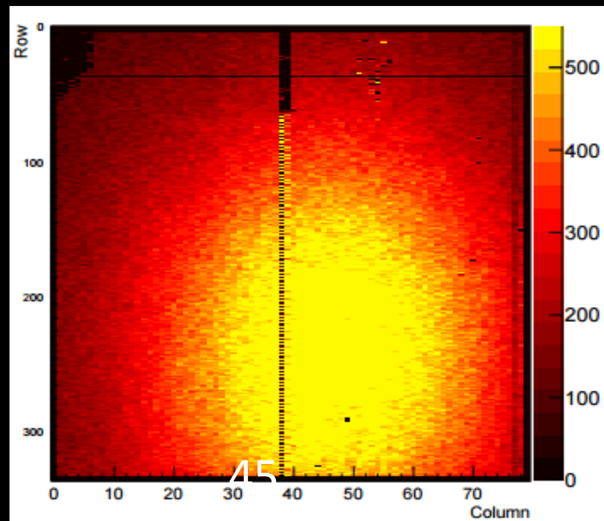

The key to fabrication: plasma etching

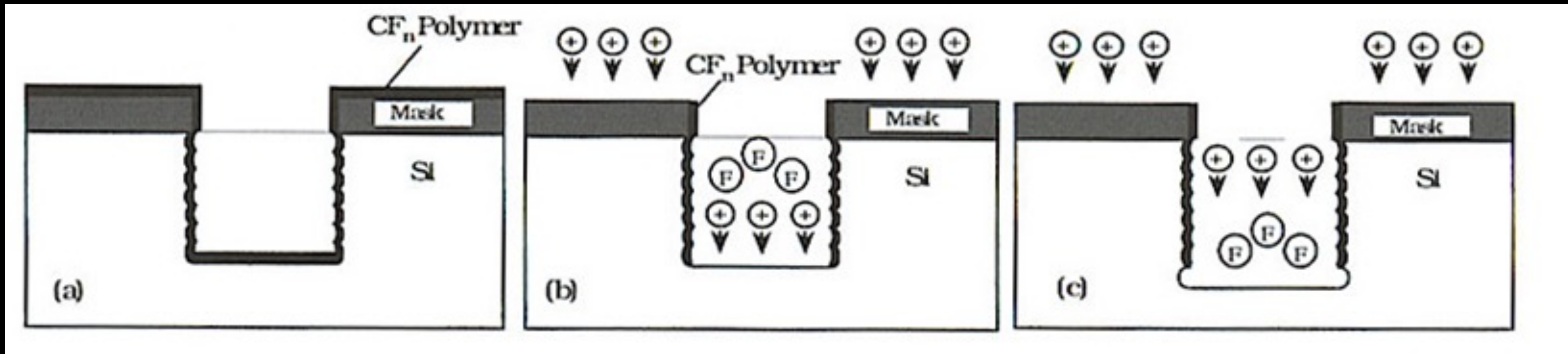

BOSCH PROCESS: alternating passivation (C_4F_8) and etch cycles (SF_6);

- Within the plasma an electric field is applied perpendicular to the silicon surface.
- The etch cycle consists of fluorine based etchants which react with silicon surface, removing silicon. The etch rates are ~1-5µm/minute.
- To minimize side wall etching, etch cycle is stopped and replaced with a passivation gas which creates a Teflon-like coating homogenously around the cavity. Energetic fluorine ions, accelerated by the e-field, remove the coating from the cavity bottom but NOT the side walls.

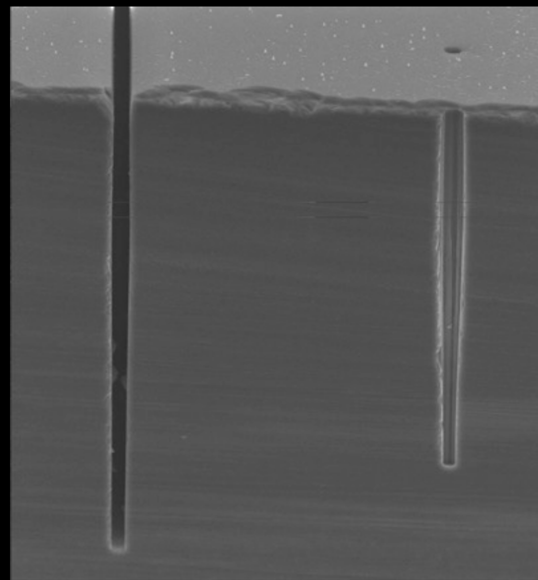

724104 25KV X300 100µm

Slide from J. Hasi

Developments in Bulk Micro-Fabrication

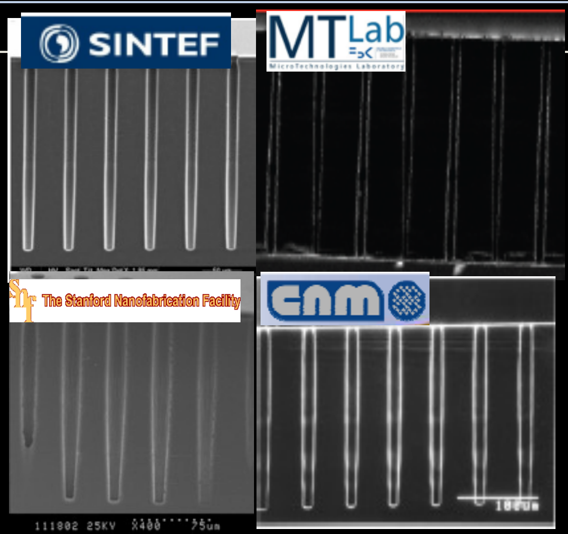

11:1
1997

24:1
today

40-60:1

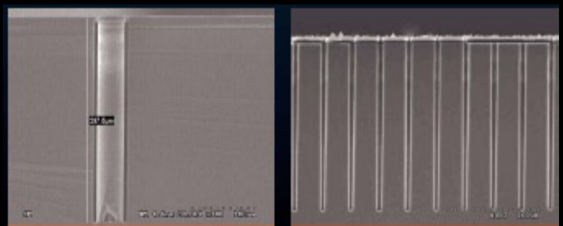

60:1 Aspect ratio 3D Via contacts
Width: 5 µm Depth: 300 µm

40:1 Aspect ratio deep micro holes
diameter: 4 µm Depth: 160 µm

110:1!!!

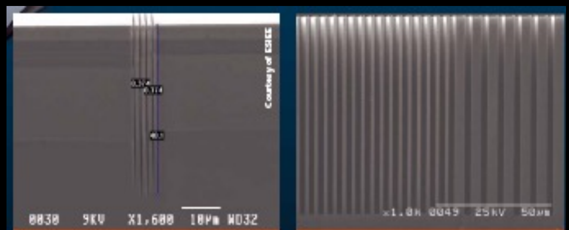

110:1 Aspect ratio of sub micron trenches

60:1 Aspect ratio trenches for Power Device application
Width: 1.4 µm Depth: 84 µm

ALCATEL Micro Machining Systems

← Deep Reactive Ion Etching

Cryo-etching →

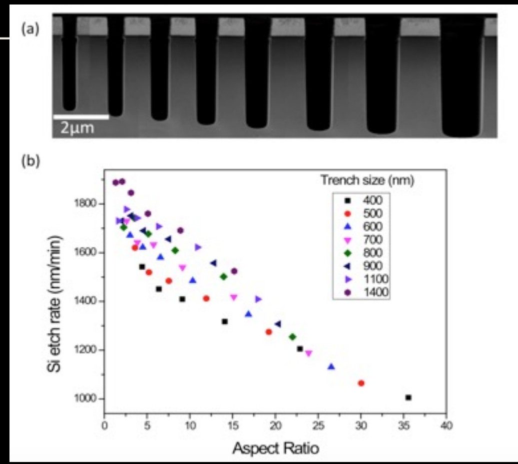

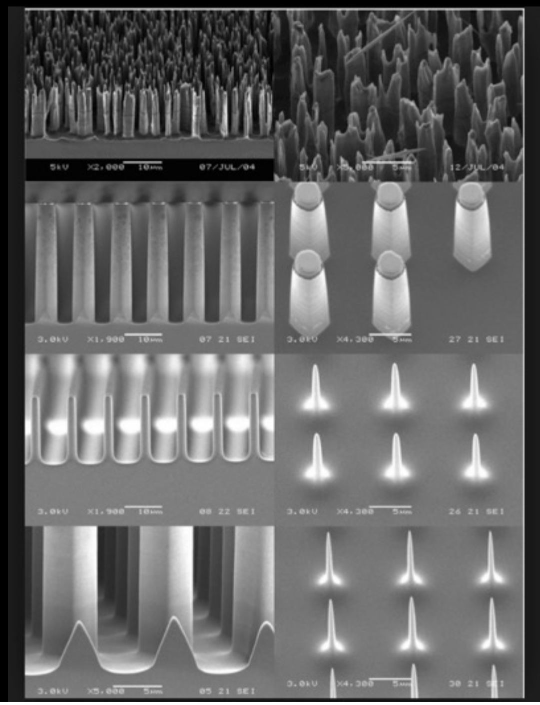

Cinzia Da Via, Stony Brook USA and The University of Manchester, UK– 2022

3D Detectors and applications

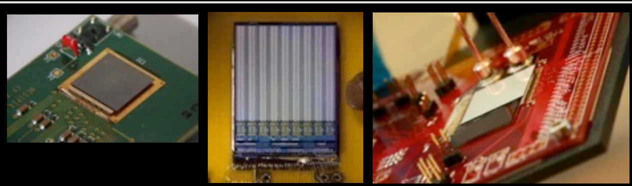

ATLAS FE-I3
ATLAS FE-I4 (with micro-channels)
AFP
Medipix/Timepix
CMS

LHC-Upgrades

- GaAs
- CdTe
- Diamond

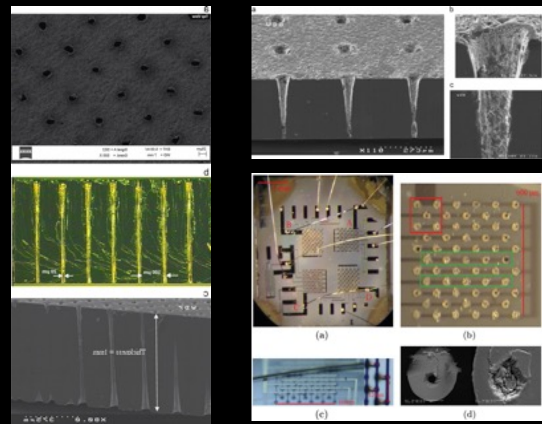

Silicon +ASIC

Consolidated

Silicon +Converter

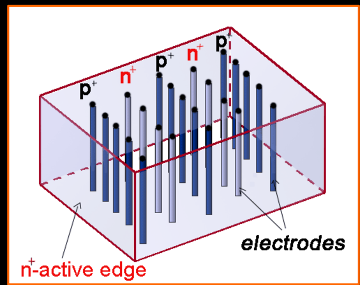

New Materials

Emerging

New Shapes

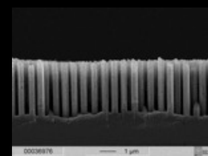

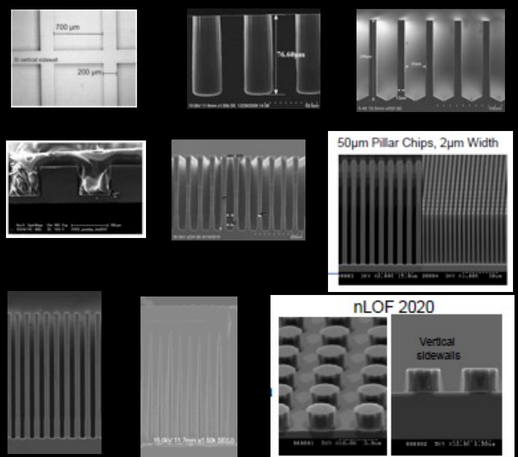

Neutron detectors

3D

- Core shell
- Curved
- Edge
- Ring..

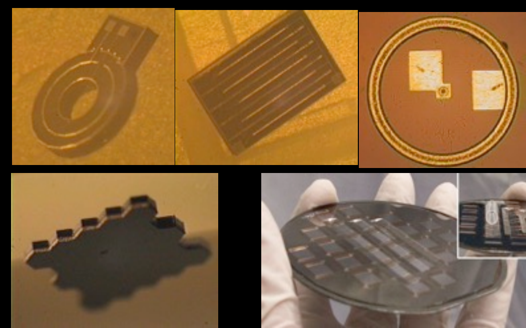

Cinzia Da Via, Stony Brook USA and The University of Manchester, UK– 2022

Concluding Remarks

The development of radiation detectors and imaging technologies has always been a crucial component in scientific discoveries and in applications like medicine and biology

… and the best has still to come..

Material From:

Status and challenges for detectors in High Energy – Ariella Cattai CERN

Status and main challenges for detectors in Synchrotron Applications - Heinz Grafsma DESY , Ralf Menk

Status and challenges for detectors in Nuclear Physics - Yacouba Diawara IAEA

Status and challenges for neutron detectors - Richard Hall-Wilton ESS

Status and main challenges for detectors at fusion facilities - Duarte Borba EFDA-JET

Status and main challenges for detectors in Hadron Therapy - Bernd Voss GSI

Status and main challenges for medical imaging detectors – Thilo Michel Erlangen

Detectors for pre-clinical imaging - Nicola Belcari INFN Pisa

Status and challenges for detectors n electron microscopy - Wasi Faruqi , Cambridge University

Status and main challenges for detectors in Astronomy and Astrophysics - Karl-Tasso Knoepfle MPI

High Z Materials - Michael Fiederle , Freiburg Univ. FMF

Natural Radiation Monitoring – Ulrich Stohlker Freiburg Univ.

Diamond Detectors- applications as radiation sensors and beam monitors – Wolfgang Lohmann DESY

Particle therapy - Patrick Le Du

Gas Detectors -Maxym Titov, Saclay

Timepix - Stanislav Pospisil, TU Prague

History -Ritam Jorder